Available online at www.sciencedirect.com
ScienceDirect
Chemie der Erde 68 (2008) 1–29
CHEMIE der ERDE GEOCHEMISTRY
www.elsevier.de/chemer

INVITED REVIEW

The significance of meteorite density and porosity

G.J. Consolmagno[a,*], D.T. Britt[b], R.J. Macke[b]

[a]*Specola Vaticana, V-00120 Vatican City State, Holy See (Vatican City State)*
[b]*Department of Physics, University of Central Florida, Orlando, FL 32816-2385, USA*

Received 3 December 2007; accepted 15 January 2008

Abstract

Non-destructive, non-contaminating, and relatively simple procedures can be used to measure the bulk density, grain density, and porosity of meteorites. Most stony meteorites show a relatively narrow range of densities, but differences within this range can be useful indicators of the abundance and oxidation state of iron and the presence or absence of volatiles. Typically, ordinary chondrites have a porosity of just under 10%, while most carbonaceous chondrites (with notable exceptions) are more than 20% porous. Such measurements provide important clues to the nature of the physical processes that formed and evolved both the meteorites themselves and their parent bodies. When compared with the densities of small solar system bodies, one can deduce the nature of asteroid and comet interiors, which in turn reflect the accretional and collisional environment of the early solar system.

Keywords: Asteroids; Density; Meteorites; Porosity; Solar nebula; Trans-Neptunian objects

1. The study of meteorite density and porosity

1.1. Introduction

On Earth, a geologist can take samples *in situ*, recognizing the stratigraphic relationship between neighboring samples, and then measure the chemical and physical properties of those samples in the lab. For studying the solar system, an analog of a stratigraphic sequence can be found in the compositions and orbital locations of small solar system bodies, which represent the relatively unprocessed material from which the major planets were formed. There are two major sources of information on the compositional diversity of the small bodies of the solar system: remote information from telescopic observations of asteroid, comet, and Trans-Neptunian object (TNO) mineralogy, and direct samples of meteorites that have fallen from the asteroid belt onto Earth, and into our labs.

The 44 compositional types, subtypes, and metamorphic grades of meteorites represent an invaluable resource of "free" geological material from asteroids that sample their mineralogy, geochemistry, and small-scale structure as well as textural and isotopic evidence of their origin and evolution. Their chemical study has been going on with a remarkable intensity since the Apollo era, coinciding with the development of highly precise devices such as scanning electron microscopes (SEMs)/microprobes and mass spectrometers, which have allowed ever finer measurements of chemical and isotopic compositions to be made at ever higher resolution on ever tinier samples. But until recently, the measurement of the physical properties of these samples has not been pursued with the same vigor. Here

*Corresponding author. Tel.: +39 06 6988 5266; fax: +39 06 6988 4671.
E-mail address: gjc@specola.va (G.J. Consolmagno).

0009-2819/$ - see front matter © 2008 Elsevier GmbH. All rights reserved.
doi:10.1016/j.chemer.2008.01.003

we review recent efforts to correct that imbalance, and show how these meteorite physical properties, in particular density and porosity, can be tied to recently determined asteroid physical properties. This study can lead us to a deeper insight into the structure of the early-forming solar system itself.

1.2. Density and porosity

Density, mass per unit volume, is one of the fundamental properties of matter. Only a limited number of parameters control a rock's density: its mass is determined by the atomic masses of the elements that make up a rock, while its volume is a function of the physical arrangement of those elements into crystalline forms, as modified by whatever flaws exist in that arrangement of elements that could cause the rock's density to deviate from a theoretical value. These flaws can include dislocations within the minerals (which in practice have a negligible effect on density), the incomplete compaction of the individual crystals in the rock, or disruptions of the fabric of the material by events such as thermal stresses or the passage of shock waves. All such voids and cracks are generally referred to as *porosity*.

The common way to determine the porosity of an object is by measuring its bulk volume V_b and grain volume V_g. Grain volume measures only the volume of solid matter in the sample, while bulk volume is based on overall dimensions and includes volume contributions from any cracks or voids that are present within the sample. Porosity is then calculated as follows:

$$P = \left(1 - \frac{V_g}{V_b}\right) \times 100\%.$$

Alternatively, if bulk density $\rho_b = M_m/V_b$ (where M_m is the mass of the meteorite) and grain density $\rho_g = M_m/V_g$ are determined, porosity can be calculated by

$$P = \left(1 - \frac{\rho_b}{\rho_g}\right) \times 100\%.$$

Like density, mineralogy is also a function of the composition and arrangement of atoms within a substance. But while mineralogy and density both depend on the same variables, there is not a unique mapping between them. Different minerals can have the same densities, while a given mineral can be a solid solution of different cations (such as Fe and Mg) and thus exhibit a range of different densities. Still, most meteorites have a relatively simple mineralogy, fixed by the equilibrium chemistry of elements whose relative abundances are usually not too different from solar abundances, formed at relatively uniform (and low) pressures and temperatures. Thus one might expect that a meteorite's density could provide at least a zeroth-order indication of its mineral composition.

Britt and Consolmagno (2003) reviewed the measurement of meteorite densities that had been measured through the year 2001. Until the 1950s, most meteorite density values were found casually as a part of the description of individual falls. In most of those cases, the authors did not outline the method used to make the measurement, presumably using the standard geological technique of weighing the sample first in air and then suspended in water. This method gives a quick estimate of the bulk density of the sample, but does not take into account any penetration of the water into the pore space and, of course, carries with it the risk of contamination and weathering that can result from dipping meteorites into water.

The first systematic study of meteorite porosity was presented by Keil (1962), although earlier papers by Alexayeve (1958) and Stacy et al. (1961) had published porosities for six and eight meteorites, respectively. Keil measured 48 meteorites with the uniform technique of immersion into water to find a bulk density, and into carbon tetrachloride (taking steps to insure that it saturated the pore spaces) to find the grain density. In 1960s Brian Mason also measured the grain densities of 70 meteorites with carbon tetrachloride, but most of these were not published until the Britt and Consolmagno (2003) compilation.

After a gap of 20 years, a new series of density and porosity measurements were conducted in the 1980s. At the National Institute for Polar Research in Japan, 40 meteorites from their Antarctic collection were measured for density and porosity (Matsui et al., 1980; Miyamoto et al., 1982; Yomogida and Matsui, 1981, 1983), while researchers at the Geological Survey of Finland measured bulk densities (and, in some cases grain densities and porosities) for the largest sample set up to that time, 489 pieces (most of them only a few grams) of 368 different meteorites (Kukkonen and Pesonen, 1983; Terho et al., 1993; Pesonen et al., 1993); a similar, if smaller, study was carried out in Leningrad (Guskova, 1985).

The first measurements of meteorite bulk densities using glass beads instead of water (see below) were reported by Consolmagno and Britt (1998). Since then, a combination of glass bead (or digital imaging) and gas pycnometry methods have been used by us and a number of other workers (Flynn and Klock, 1998; Moore et al., 1999; Flynn et al., 1999; Wilkison and Robinson, 2000; Kohout et al., 2006; Smith et al., 2006; McCausland et al., 2007) to measure meteorite densities and porosities.

Besides volume measurements, other techniques for determining porosity directly include point-counting void spaces visible in SEM backscatter images or inferring porosity from the measurement of sound

speeds within the samples (Corrigan et al., 1997; Britt and Consolmagno, 2003; Strait and Consolmagno, 2002a, 2005).

As of the end of 2007, our combined database of published and, when made available to us, unpublished measurements has densities for 490 different meteorites, including 365 ordinary chondrites, 52 carbonaceous chondrites, 14 enstatite chondrites, 50 achondrites, and nine stony-irons. This represents measurements on more than 1200 different samples. However, far less than half of these meteorites have been measured in a common, uniform, and reliable way for both bulk and grain densities to provide accurate porosities. Thus there still remains a significant need for further measurements, especially for meteorites other than ordinary chondrites.

1.3. Measuring bulk volume

For irregularly shaped samples (typical of meteorites), measurement of bulk volume poses numerous challenges. Cutting an irregular rock can produce a shape whose volume can be easily calculated geometrically, but it has always been desirable to measure the volume of a sample without altering or destroying it in the process. The classical way to measure the volume of an irregularly shaped object is to immerse it in an incompressible fluid and then measure the volume of the displaced fluid. A variation on this technique is to weigh the sample first in air, and then suspended in water; from the difference in the weights, resulting from the buoyancy of the sample in water, the density of the sample relative to water can be determined.

However, there are many problems involved in immersing a meteorite in any fluid, especially water. First, the fluid may chemically react with the meteorite, thus altering it, which is particularly problematic with water. Second, the fluid may leave residues on the sample which may be difficult or impossible to remove and could complicate or invalidate any future analysis of the meteorite. Finally, pore space may be permeable to fluids to an unknown degree; certainly, the longer a sample is immersed, the more the fluid penetrates the pore space and the less reliable the result becomes as a measure of bulk volume. Some workers have attacked the bulk volume measurement problem in other, more creative ways (see summary in Britt and Consolmagno, 2003). One method is to pack the meteorite in clay and form the clay into a shape whose volume is easily determined. The meteorite is then removed, the clay is remolded, and its new volume measured; the volume of the meteorite is the difference between the two measured volumes. This approach leaves clay on the meteorite which may be difficult to remove and has the potential for reactivity and contamination. One can first wrap the meteorite in a thin plastic sheet to protect the meteorite, but this distorts the volume measurement, especially for small samples.

If the sample is a slab, its volume can be estimated by calculating the area of a face (through pixel counting on a digital photograph or through other methods) and multiplying by the slab thickness. However, if the opposite faces are not perfectly parallel, the varying thickness across the slab must be taken into account. Generally, unless the slab has also had its edges cut, the edges are irregular and do not run perpendicular to the faces. This limits the precision of volume measurements made this way.

Smith et al. (2006) and McCausland et al. (2007) are developing three-dimensional (3-D) laser imaging techniques for measuring volume. Their work has produced results consistent with other methods and is scalable to accommodate large and small fragments (down to $\sim$1 cm^3). However, currently this method requires 15–30 min to scan a meteorite and 2–4 h of labor-intensive, skilled processing to reduce the data and achieve a single measurement, making it impractical for use on large numbers of samples.

Consolmagno and Britt (1998) outlined a method in which small ($\sim$40 μm diameter) glass beads serve the same function as an incompressible Archimedean fluid. Because the beads are solid rather than liquid, they will not leave residue, and since glass is chemically stable they have no chemical reactivity. The size of the beads is large relative to the scale of meteorite pores, so unless the pores are unusually large, intrusion into pore space is not a problem. Another appeal is the fact that the beads, manufactured in bulk for industrial use, are available cheaply and in large quantities. The ''bead method'' is a quick, reliable, non-destructive method for bulk volume measurement that is rapidly finding uses in fields beyond meteoritics.

The procedures for the glass bead method are quite similar to those employed for fluids. First, the density of the beads is determined by filling a flat-topped cup of known volume with beads and measuring the mass. Before massing, the beads are encouraged to settle, either by vigorous shaking of the cup (a mechanical vibrating platform on a timer is often used) or by tapping the sides of the cup, and the beads are leveled flush with the top of the cup by scraping off the excess. To obtain good statistics for determining measurement uncertainty, this measurement is repeated several times, generally 10 times or more. Once the density of the beads has been determined in this way, the meteorite is placed in the cup, the beads are reintroduced, and the process is repeated. (Following the measurement, residual beads are removed from the meteorite's surface with a clean soft-bristled brush.) To minimize variations in the packing density of the beads, the same cup and settling method are used. From this second

measurement, the volume of beads can be calculated, and from that, the bulk volume of the meteorite is determined.

The bead density (ρ_B) is

$$\rho_B = \frac{M_{T0} - M_c}{V_c},$$

where M_{T0}, the total mass (cup plus beads) without meteorite, M_c is the mass of the cup and V_c is the cup volume.

The bulk meteorite volume (V_{bm}) is

$$V_{bm} = V_c - \left[\frac{(M_{TBm} - M_c - M_m)}{\rho_B}\right],$$

where M_{TBm} is the total mass (cup plus beads plus meteorite) and M_m is the meteorite mass. The term in brackets represents the volume of beads when the meteorite is submersed in the cup.

Solid powders do not behave precisely like a perfect Archimedean fluid in either their flow or settling properties, which results in variations in the average density of the "Archimedean fluid" from measure to measure, although this is mitigated slightly by the uniform spherical shape of the beads. In part due to small variations in bead size, the beads do not generally pack in the optimal arrangement. Further compression is possible, especially under the compressing influence of a large (>50 g) meteorite. This problem has been noticed especially in cases where the meteorite samples were slab-shaped. To reduce this effect, two methods have been employed. One is to pre-compress the beads by vigorous shaking of the cup, forcing the beads to settle. Results of comparable quality can be obtained by employing a method designed to minimize compression; the cup is not shaken at all, but rather tapped gently on the side with the bristles of a brush just enough to cause the beads to flow into any remaining gaps. Another experiment in progress involves tightening the size sieving of the beads to minimize size variation. Significant variations in results have been also observed due to inconsistencies in the pouring technique employed. With practice, however, quite reasonable levels of repeatability have been achieved.

Environmental factors such as humidity also affect the packing behavior of the beads. While it is generally ideal to use the smallest available bead size to better approximate a fluid, the increased surface-area-to-volume ratio makes small beads more susceptible to clumping and other effects caused by atmospheric moisture condensing on their surfaces. This reduces the ability of the beads to flow evenly into gaps between the meteorite and the cup. It has often been observed that a container of beads left sitting for a period of time forms a thin surface crust. To minimize these effects, the beads need to be stirred, sifted or poured a few times before use.

Experience has shown that error is minimized by using the smallest cup into which the meteorite can fit. Measurement of the volume of the cup itself is crucial, since the meteorite volume is determined by subtracting a quantity from the cup volume. Uncertainties in meteorite volume cannot be significantly better than uncertainty in cup volume. The most common way to measure the volume of a cup is to fill it with fluid (usually water) and then determine the volume of fluid by weighing the filled cup; but most fluids produce either a concave or convex meniscus that throws off the measurement. Another method is to measure a sample whose volume can be measured independently (such as a large glass marble) and solving the equation above for V_c, the volume of the cup.

With these methods we have found that it is difficult to measure a sample volume to a precision greater than 1 cm^3. Though this is sufficiently small for larger samples, this error becomes quite significant when attempting to measure meteorite volumes that are less than 10 cm^3, i.e. for samples smaller than about 35 g assuming a typical meteorite density of 3.5 g/cm^3.

1.4. Measuring grain volume

The most effective method for measuring grain volume is ideal gas pycnometry. It takes advantage of the ideal gas law to determine meteorite volume. Helium gas offers the greatest advantage because the He atom is so small that it will quickly and easily penetrate any cracks in the sample, and because He is chemically inert.

Typically, two sealed chambers of known volumes are connected through a valve. The meteorite is placed in one chamber, which then has He introduced into it while the connecting valve is closed. The second chamber is held at a different pressure from the first chamber. The simplest procedure is to raise the pressure of the meteorite's chamber to well above ambient room pressure (typically a pressure near 1.5 atm is used); then the second chamber may either be evacuated or simply be purged with He and maintained at the local ambient pressure. After pressure in the first chamber is measured, the valve is opened, allowing the gas to flow into the adjacent chamber until pressure in both chambers has equalized. In the case of previously evacuated chambers, the ideal gas law dictates the relationship between pressure and volume:

$$P_i(V_A - V_{gm}) = P_f(V_A + V_B - V_{gm}),$$

where P_i and P_f are initial and final pressure, respectively; V_A and V_B are volumes of the two chambers, respectively (where chamber A is the one containing the meteorite); and V_{gm} is the grain volume of the meteorite. Solving for the grain volume of the

meteorite yields:

$$V_{gm} = V_A - \frac{P_f}{(P_i - P_f)} V_B.$$

For the case where the second chamber is initially at atmospheric pressure rather than evacuated, local atmospheric pressure must be taken into account, but this can be easily accommodated by measuring all pressures as overpressures relative to atmospheric rather than as absolute pressures. With pressures measured this way, the calculations are identical to that for an evacuated chamber.

For hand-sized samples, evacuation of the second chamber is not necessary in order to obtain reliable measurements. A typical commercial pycnometer (Quantachrome) yields grain volume measurements repeatable to within $\sim 0.02\,cm^3$ without employing a vacuum pump.

Indeed, for meteorites it is preferable to avoid using a vacuum pump, because there is always the chance of sample contamination originating from the pump itself. Worse, the removal of moist terrestrial air from the interior of the meteorite has been seen in the case of CI chondrites to promote the migration of water-soluble compounds from the interior of the meteorite, thus accelerating terrestrial weathering (Gounelle and Zolensky, 2001). In addition, the chamber would need to be evacuated with each new sample, adding to the time it takes to complete the measurement.

2. Meteorite density and porosity data

2.1. Ordinary chondrites

Ordinary chondrites represent by far the most numerous type of stony meteorite, both in fall and find statistics, representing 74% of all meteorites seen to fall and 92% of those found in the relatively unbiased Antarctic collections (McBride, 2002). Likewise, they are the set of meteorites most widely measured for density and porosity, with density data reported for 860 samples of 365 different meteorites, and reliable porosities for 131 meteorites. The average densities and porosities for each group are tabulated in Table 1. (Unless noted otherwise, the plus/minus values in this section refer to variation from meteorite to meteorite, not measurement error.)

A number of trends stand out. Not surprisingly, the grain densities of freshly fallen ordinary chondrites closely follow the iron content, with H chondrites more dense than L and LL types, completely consistent with their mineralogy. We note that for fresh falls, grain density alone can distinguish between H and L types, but there is a significant overlap between the L and LL classes. Bulk densities also decrease with decreasing iron content, but with more overlap among the different classes. Variations in porosity from sample to sample show up as differences in bulk density, of the same order as the differences due to iron composition from H to L to LL classes, thus blurring the differences due to iron content.

The grain densities of finds (not counting Antarctic finds) are significantly different from the grain densities of falls. For example, among the H class finds, the grain density is only $3.55\,g/cm^3$; for L chondrites, it drops to $3.41\,g/cm^3$. Given the typical error of $0.1\,g/cm^3$ in the measurements, for finds density is no longer a robust discriminant between H and L class meteorites. (Too few LL meteorite finds have been measured to make any statistically significant statement, but the few data points in hand also follow this trend.) Notably, the average grain densities of Antarctic finds is similar to that of fresh falls.

Given grain and bulk densities, porosities can be computed. The average porosity measured for all ordinary chondrite *falls* is $7.4 \pm 5.3\%$, with L chondrites tending to be slightly less porous than H and LL chondrites. However, among *finds*, the average porosity is only $4.4 \pm 5.1\%$, a spread from sample to sample that ranges from fall-like porosities down to zero porosity.

These density and porosity trends are consistent with weathering studies of ordinary chondrites. One would expect that weathering could occur rapidly at first, as moisture enters the sample through the microcracks that we detect as pore spaces. For ordinary chondrites, the weathering product is primarily iron oxides produced by the reaction of terrestrial oxygen with the abundant small metallic grains characteristic of these meteorites. The oxides of iron (typically goethite) are about half as dense as the original metal grains ($3.3–4.3\,g/cm^3$ for geothite versus $7.6–7.8\,g/cm^3$ meteoritic iron) and thus expand into the pore spaces. Once the cracks are

Table 1. Ordinary chondrite average densities (g/cm^3) and porosities

Class	Average grain density (falls)	±	Average bulk density	±	Average porosity (falls) (%)	± (%)	Average model porosity (%)	± (%)
H	3.72	0.12	3.42	0.18	7.0	4.90	9.9	4.7
L	3.56	0.1	3.36	0.16	5.6	4.70	7.5	4.3
LL	3.54	0.13	3.22	0.22	8.2	5.50	9.9	6.1

completely filled, the grain volume matches the bulk volume and the porosity goes to zero. At that point, weathering can only proceed very slowly, as water and oxygen can reach the remaining metal only by diffusing through the minerals themselves. Bland et al. (1996, 1998), correlating the oxidation state of iron (as measured by Mössbauer spectroscopy) with the terrestrial ages of the samples, have observed just such a two-stage transformation, first rapid then much slower, in the ordinary chondrites.

If weathering products act first to fill void spaces within the meteorite, one would expect that this first stage of weathering at least should not significantly alter the mass or outside shape of meteorites. If that is so, then there should be essentially no difference between the bulk densities of falls and finds. In fact, in our database they are indeed identical. For H meteorites falls, the average bulk density is $3.42 \pm 0.19\ g/cm^3$; for finds, it is $3.42 \pm 0.16\ g/cm^3$. Among L meteorites, fall bulk densities average $3.37 \pm 0.18\ g/cm^3$, while finds average $3.37 \pm 0.10\ g/cm^3$. (Again, there are too few LL meteorite finds measured to make statistically significant statements.)

If weathering does not alter ordinary chondrite bulk densities then *model* porosities can be calculated for chondritic meteorites by assuming that their initial, unweathered grain densities were identical within each class, fixed only by their original pristine mineralogy, while their bulk densities were unaffected by weathering (Consolmagno et al., 1998). In this way the large number of chondrite finds can be included in our statistics. This also corrects for weathering within the falls. (On average the difference between the model and measured fall porosities is about 1% porosity.) And since calculating grain densities removes the need to actually measure grain densities, which requires more elaborate equipment than the simple bead method for bulk densities, using model porosities significantly increases the number of meteorites for which porosities can be derived and included in our statistical set.

Using the average modal mineralogy for the H, L, and LL ordinary chondrites classes (McSween et al., 1991), we calculate model grain densities of $3.78\ g/cm^3$ for H chondrites, $3.62\ g/cm^3$ for L chondrites, and $3.57\ g/cm^3$ for LL chondrites. With these values, model porosities have been calculated for 324 ordinary chondrite meteorites (Table 1). (By comparison, only 68 relatively unweathered falls have had porosities measured directly.) McSween et al. (1991) also note a variation in the composition, especially the metal content, among meteorites within a given class; given their reported variations, we estimate that these calculated grain densities are good to plus or minus $0.03\ g/cm^3$, and thus the model porosities are accurate to 0.6% porosity.

What is most remarkable about the trends among meteorite classes in model porosity is in fact the lack of trends. The average model porosity for all ordinary chondrites is $8.9 \pm 4.9\%$. For H chondrites alone, it is $9.9 \pm 4.7\%$; for Ls, $7.5 \pm 4.3\%$; for LLs, $9.9 \pm 6.1\%$. We note that the L chondrites do appear on average to be lower in porosity than the other groups, albeit with a significant overlap (the plus/minus represents variations in porosity from meteorite to meteorite, not uncertainty in the measurements). Most remarkably, these average porosities are uniform over sample mass, petrographic grade, and nearly uniform with shock state (Figs. 1–3 and Tables 2, 3).

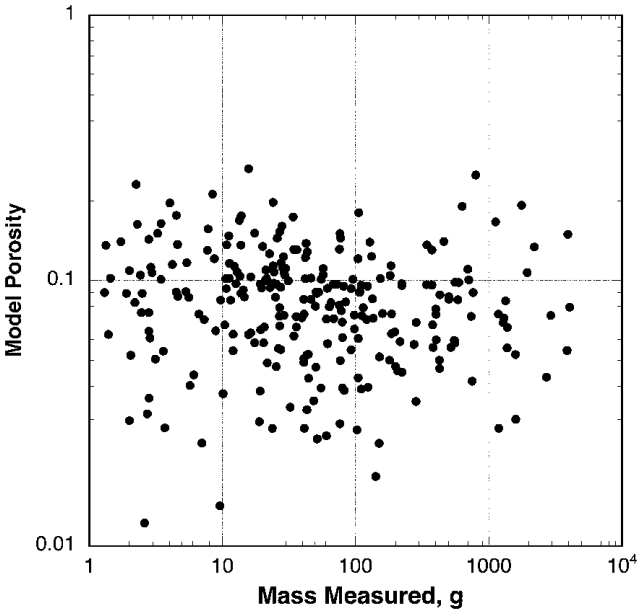

Fig. 1. Model porosity (volume fraction) of ordinary chondrites as a function of sample mass, in grams. There is no visible trend for the average porosity (the slope of a line fit to these points is zero). More surprisingly, there is also no obvious change in the spread of the data around the average over this range of sample masses, indicating that the variation in porosity from sample to sample is uniform across four orders of magnitude in size. Pore spaces in these samples are distributed homogeneously on a scale much smaller than the smallest samples measured.

2.2. Carbonaceous chondrites

Carbonaceous chondrites are far less numerous than ordinary chondrites, and their densities and porosities far less well studied. In our database we have densities for 52 different meteorites, but these are spread among seven classes; only CM, CV, and CO meteorites have 10 or more meteorites with any sort of density measurements. Furthermore, only 17 of those 52 meteorites have hand samples that have been measured simultaneously for both grain and bulk density, for which a porosity can be derived. Thus only the most general of statements can be made about their densities and porosities.

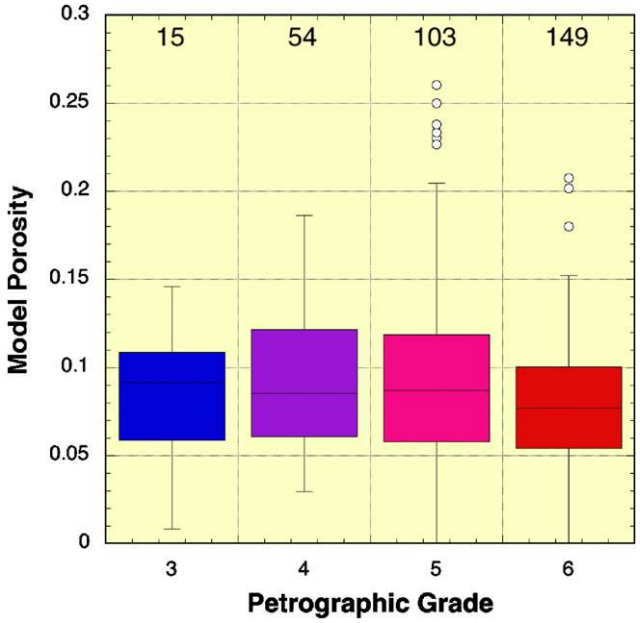

Fig. 2. Model porosity (volume fraction) of ordinary chondrites as a function of petrographic grade. There is no difference in porosity across petrographic (metamorphic) grades, indicating that the porosity was emplaced after the samples experienced metamorphism. Fifty percent of the data lie within the shaded bars, with the median indicated by the horizontal line within the bar. The vertical "error bar" lines above and below the shaded bars indicate the range of the remaining upper and lower quartiles of the data, except for three-sigma outliners indicated as individual points. The number of meteorites measured for each petrographic grade is indicated by the numbers above the bar.

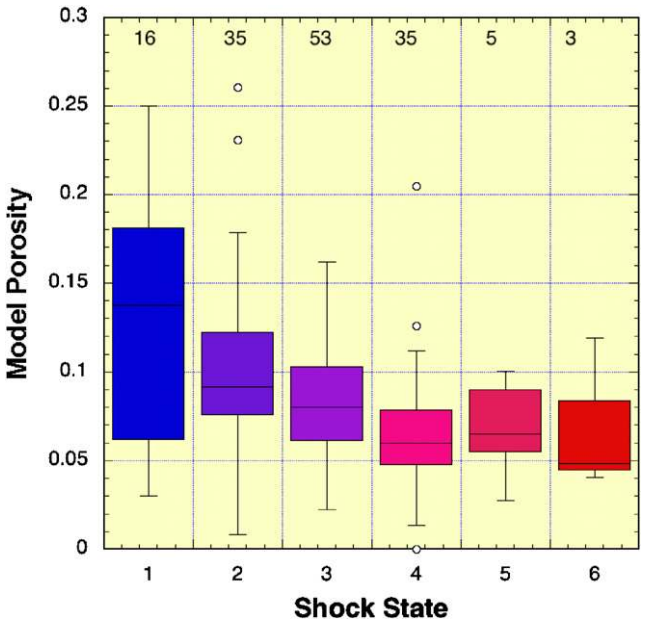

Fig. 3. Model porosities of ordinary chondrites as a function of shock state; data ranges are as described for Fig. 2, with the number of data points in each shock state indicated above the bars.

Table 2. Petrographic grade vs. model porosity

Petrographic grade	Average model porosity (%)	± (%)
3	9.2	3.5
4	9.3	4.0
5	9.7	5.4
6	8.1	4.6

Table 3. Shock state vs. model porosity

Shock state	Average model porosity (%)	± (%)
1	13.0	6.8
2	10.0	5.3
3	8.3	3.1
4	6.5	3.7
5	6.8	2.9
6	6.9	4.3

Although carbonaceous chondrites come in a wide variety of classes, in terms of densities they can be divided into two groups (see Table 4). The higher-density carbonaceous chondrites are the anhydrous groups, such as the CV, CO, and CK meteorites, plus the hydrated but metal-rich CR class. These meteorites' grain and bulk densities lie within the range for ordinary chondrites. The average grain density is 3.50 ± 0.15 g/cm^3, similar to that of L and LL chondrites; the average bulk density of 2.92 ± 0.2 g/cm^3 is about one sigma lower than LL chondrites, not sufficiently different that one could use bulk density alone to discriminate reliably between the two groups.

Within these groups, however, there are significant differences in porosities among the anhydrous C meteorites. Five of the eight CV and CK meteorites (the two classes are thought to be closely related) measured in hand sample for porosity to date are more than 20% porous, while five of the six CO meteorites with measured porosities are under 15% porous.

Notably, all five of the low porosity CO meteorites (along with the one CR with a reliable porosity, Acfer 097 – porosity 14%) are finds, while the one fall, Warrenton, has a porosity of 26%. The higher porosity of this meteorite is reflected in its higher grain density, 3.7 g/cm^3 compared to 3.3–3.5 g/cm^3 seen in the other CO samples. Both trends are consistent with terrestrial weathering products filling pore spaces in the CO finds. Greenwood and Franchi (2004) have shown that terrestrial weathering significantly alters the carbon isotopes in CO meteorites, which they attribute to the presence of carbonates formed by the evaporation of carbonate-rich terrestrial water that has been taken up by the meteorite (as first suggested by Ash and Pillinger, 1995). Presumably these carbonates are filling void spaces in the meteorite, lowering its porosity.

Table 4. Carbonaceous chondrite average densities (g/cm^3) and porosities

Class	Average grain density	±	Average bulk density	±	Average porosity (%)	± (%)
CI	2.46	0.04	1.6	0.03	35	–
CM	2.90	0.08	2.25	0.08	23.1	4.7
CO	3.41	0.23	3.03	0.19	10.8	9.1
CVo	3.30	0.15	2.79	0.06	21.8	1.7
CVr	3.45	0.09	0.12	0.25	9.7	4.9
CK	3.58	0.09	2.85	0.08	21.8	2.2

However, such weathering has not had a similar effect on the porosity of finds in other carbonaceous chondrite classes. There is no distinction between the porosity of falls and finds among the CV and CK class. Though there is a notable spread in porosity in the CV class, the meteorites with lower porosities are Leoville (13%), a find, and Vigarano (6%), a fall; the other CVs with reliable porosity measurements are Allende (fall, 23.0 ± 5% based on 48 measurements) and Axtell (find, 21 ± 2% based on two measurements). The three measured CK meteorites range in porosity from 21% to 24%; two are falls, one a find.

Krot et al. (1995) have divided the CV class into oxidized and reduced subgroups. The two high porosity CVs, Allende and Axtell, are also members of the oxidized group, while the two low porosity CVs, Leoville and Vigarano, belong to the reduced subgroup. MacPherson and Krot (2002) noted that reduced CV meteorites appear to have been compacted in their parent body and suggested that they ought to be significantly lower in porosity than those of the oxidized group. While the agreement of the data with this suggestion is encouraging, we caution against making any definitive statement about trends based on only four samples. But we note, as seen in Table 4, that even when one includes density data from other CV samples for which porosity values are not yet available, the grain densities of the oxidized CVs are still significantly higher, and the bulk densities lower, than the reduced group, which is consistent with this hypothesis.

The hydrated CM and CI meteorites are significantly lower in density than any other meteorites, with grain densities well below 3 g/cm^3 and bulk densities near or below 2 g/cm^3. The values for CMs are relatively uniform across samples and measurement techniques. Fourteen measurements of seven different CMs (six from Murchison and another three from Murray) yield an average grain density of 2.82 ± 0.13 g/cm^3; the bulk density (13 measurements of six meteorites, again including six Murchison measures) average is 2.13 ± 0.19 g/cm^3. Only for Murchison and Murray (along with Orgueil) are there measures of both grain and bulk densities (found via the glass bead/He pycnometry methods) of the same sample, from which a reliable porosity can be derived; the average porosity of Murchison (based on three samples only) is 22 ± 2%, while the sole porosity measure for Murray is 28%. Note, however, that while the point-counting method (Corrigan et al., 1997) yields a similar porosity of 23% for Murchison, it gives a porosity of only 4% for Murray.

For the CI chondrites the reported densities depend strongly on the techniques used to make the measurements. Helium pycnometry yields grain densities consistently higher than those found by saturating the samples in carbon tetrachloride or water. By contrast, liquid immersion methods yield significantly higher bulk densities than the bead method – indeed, in the same range as the grain densities measured via saturation by liquids. Thus, measurements based on the traditional fluid immersion methods would suggest that the CI Orgueil would have almost no porosity (with grain and bulk densities both around 2.2 g/cm^3) while the same meteorite measured with pycnometry and beads implies a porosity of 35% (grain density 2.4, bulk density 1.6 g/cm^3; see Discussion). Orgueil is the only CI for which glass bead and pycnometry data are available, but we note that its low bulk density of 1.6 g/cm^3 is matched by the bulk density of the unusual C meteorite Tagish Lake.

2.3. Enstatite chondrites

Even more than with carbonaceous chondrites, finding trends among the enstatite chondrites is hobbled by the sparsity of data. In our database only 14 enstatite chondrites have had their grain densities measured (averaging 3.65 ± 0.07 g/cm^3); 10 have had bulk densities measured (averaging 3.46 ± 0.16 g/cm^3).

In nine cases, both kinds of density were measured for the same sample, from which a porosity can be derived. All but two of these porosity measurements were made by Consolmagno et al. (2007); the two previous literature measurements agree well with our measurements. The measured porosities appear to cluster into two groups, with six meteorites having low porosities (0.3–6.4%) and three others with 11.7%, 12.3%, and

12.6% porosity. Both groups include falls and finds; both include samples from the EL and EH subclasses.

The EL and EH subclasses (Sears et al., 1982) were originally defined in terms of high (EH) and low (EL) iron and siderophile contents, though later work has suggested that the differences in iron content may not be as characteristic of the groups as first thought. A difference in iron content would presumably manifest itself in the grain densities of the meteorites, and indeed we find on average a slightly higher grain density (3.70 ± 0.03 g/cm^3) for EH meteorites compared to EL samples (averaging 3.61 ± 0.07 g/cm^3). The difference is small, however; and given the sparse data set, it is not clear if it is significant. Indeed, both we and Guskova (1985) found a higher grain density for the EL chondrite Pillistfer than is seen in four of the six EH samples.

2.4. Achondrites and other meteorites

Only five meteorites of the "primitive achondrite" group have been measured for porosity, two brachianites and three winonaites. Not surprisingly, given the chemical similarities with the ordinary chondrites, their densities and porosities closely resemble ordinary chondrites: average grain density of 3.63 ± 0.17 g/cm^3, average bulk density 3.23 ± 0.18 g/cm^3, average porosity 11.5 ± 3.6%. Even fewer measurements have been made for ureilites; their average grain density of 3.34 ± 0.09 g/cm^3 is based on only three measurements, while nine samples (of five different ureilites) have been measured for bulk density, giving an average of 3.14 ± 0.22 g/cm^3. Only two samples have both grain and bulk densities; in both cases, the porosity is low but the formal error large. One can only say that the porosity is probably less than 6% and may in fact be zero. Three aubrites (enstatite achondrites) have hand-sample porosities measured, showing no obvious pattern (porosities of 4%, 13%, and 21%).

Even among the more numerous basaltic achondrite meteorites (Table 5), the situation is one of too few data to make any strong statements at present. For the HED class, 27 meteorites have been measured, about half of them eucrites; only five diogenites and eight howardites are in our database. Porosities based on grain and bulk densities from the same sample are even rarer. No such porosities are yet available for any howardite, and only two diogenite porosities have been measured. The situation for the eucrites is only slightly better, with seven porosities available; they range from 1% to 19%.

For the SNC class, the only nakhlite measured is Nakhla itself (three different samples) and the only chassignite measured is Chassigny itself (only one sample). Eight pieces of five different shergottites have been measured.

One interesting result for the basaltic achondrites is that, because of the great interest in these meteorites, the mineralogy is well known not only for each general class but often for individual falls (Kitts and Lodders, 1998; Lodders, 1998). From that mineralogy, a model grain density and model porosity can be computed for those samples, even where a grain density has not been measured directly. Since these samples do not contain significant metallic iron, weathering should not alter the samples to the degree seen in the ordinary chondrites. However, where measurements for particular basaltic achondrites do exist, in some cases the difference between the model and measured grain density values are significant. Usually the measured grain densities are lower than the model densities and correspondingly, the model porosities are higher than the measured values.

Beyond the work of Henderson and Perry (1954) on the density of meteoritic nickel-iron, little work has been done on the density or porosity of iron and stony-iron meteorites. Presumably, any variation of an iron meteorite's density from that of pure nickel-iron (7.8 g/cm^3) could be used to infer the abundance of sulfide or other inclusions. And the porosity of metal-rich breccias such as mesosiderites could in the future put constraints on the brecciation and relithification process.

3. What density and porosity tell us about meteorites

3.1. Introduction

Just as the oxidation state of iron and the distribution of oxygen and other isotopes allow us to understand the

Table 5. Basaltic achondrite average densities (g/cm^3) and porosities

Class	Average grain density	±	Average bulk density	±	Average porosity (%)	± (%)	Average model porosity (%)	± (%)
Howardite	3.22	0.16	2.97	0.16	–	–	11.30	4.80
Eucrite	3.18	0.05	2.9	0.13	9.30	6.20	9.70	3.80
Diogenite	3.46	0.12	3.23	0.15	2.50	2.20	7.20	4.30
Shergottite	3.39	0.03	3.03	0.28	13.60	9.50	8.80	7.80
Nakhlite	3.29	0.09	3.15	0.07	5.70	3.50	5.40	0.10
Chassignite	3.72	0.04	3.4	0.11	6.80	2.20	5.40	0.20

compositional history of meteorites (and their parent bodies), so the density and porosity of meteorites are our primary tools to understand their physical history.

From the discussion of the density and porosity data above, certain trends are immediately apparent. The H, L, and LL chondrites have essentially indistinguishable porosities and so one can conclude that they have undergone very similar physical processes, and these events occurred after the compositional nature of these classes were fixed. Furthermore, since their porosity shows no correlation with petrographic grade, as is illustrated in Figs. 2, one is led to the rather startling conclusion that whatever determined their porosity must have occurred independently of whenever their metamorphic states were determined. Given that metamorphism would presumably alter porosity, one can only conclude that the pore-forming events for in the ordinary chondrites occurred after the metamorphic events.

The correlation of shock state with porosity is more subtle. Table 3 indicates a slight decrease of porosity with shock state, but examining the data (as illustrated in Fig. 3) indicates that in fact over all shock states, the bottom quartiles of porosity measurements end at about 6% porosity. The lower shock states have a higher upper range, and hence a higher average value. Increasing shock appears to compact and remove porosity from only the more porous samples. Shock events, as we will argue below, may ultimately produce (or at least contribute to) the observed porosity; if so, a certain "baseline" of 6–10% porosity appears to result, independent of the strength of the shock.

The enstatite chondrite and the primitive achondrite data are too sparse to make a similarly strong statement, but the data in hand are certainly consistent with the possibility that they also participated in the same physical history as the ordinary chondrites, and obtained their porosity after their compositional, metamorphic, and shock states had been fixed. The other achondrites also appear to have similar porosites though the data are sparse. This is true in spite of the obvious difference in their physical histories (such as the melting and recrystallization that they experienced) and the greater physical strength resulting from their igneous origin. The fact that they experienced igneous evolution, unlike the chondrites, points to an origin under very different circumstances: perhaps a larger parent body, a physically different location from the chondrites, or a different time in solar nebula history when radioactive or other heat sources were more prevalent. But it is not clear that this difference appears to extend to their physical histories as well.

However, whereas the other meteorites tend to have porosites averaging 10% or less, the overwhelming majority of carbonaceous meteorites (with the notable exception of CO finds and reduced CVs) have porosities of 20% or more. Nonetheless these samples are generally strong, well-lithfied samples. (We do have in our collections some highly friable samples of volatile-rich meteorites, notably the CI meteorite Orgueil and the unusual C meteorite Tagish Lake; but even these meteorites were able to survive passage through our atmosphere as recognizably solid, individual samples.) The contrast between the porosities of these meteorites and the ordinary chondrites argues that the carbonaceous chondrites are in a very different physical state and likely have undergone a very different physical history than the other chondrites, presumably in a very different part of the solar nebula.

3.2. Where are the pore spaces?

To understand what porosity can tell us about the physical history of the meteorites, it is useful to understand just where the pore space is located within a given sample. Does it occur as large voids between grains? As sub-micron voids between the tiny grains in the ground mass? As microcracks permeating the meteorite? One obvious way to answer this question is to examine the meteorite fabric directly in SEM backscatter images. As noted above, Corrigan et al. (1997) for carbonaceous chondrites and Strait and Consolmagno (2002a, 2005) for ordinary chondrites have reported porosities based on point-counting the voids visible in such images. Strait and Consolmagno (2002b) reported a surprising homogeneity in porosity on the scale of a single SEM image (several hundred microns) and across a thin section. For ordinary chondrites, this method can in general derive porosities that are consistent with those measured in hand samples.

Most of the void space visible in SEM images of ordinary chondrites occurs as a network of microcracks that cut across grain boundaries (Fig. 4). Such microcracks are produced by the passage of shock waves through a solid medium; the passing wave first compresses, then decompresses, the medium, leaving the cracks in its wake (DeCarli et al., 2001; Bowden, 2002). The source of these shock waves is, presumably, impact cratering on the meteorite parent bodies. At the very least, every meteorite must have experienced some shock during whatever event removed it from its parent body, and during its final deceleration upon hitting the atmosphere and landing on Earth. Note that the creation of microcracks is not strongly linked to the strength of the shock; even relatively mild shocks will produce microcracks.

Is it possible that the microcracks seen in the SEM images are merely artifacts from cutting and mounting the thin section? This is unlikely on two counts. First, if the thin-sectioning was a significant cause of the cracking, then one would expect point-count porosities

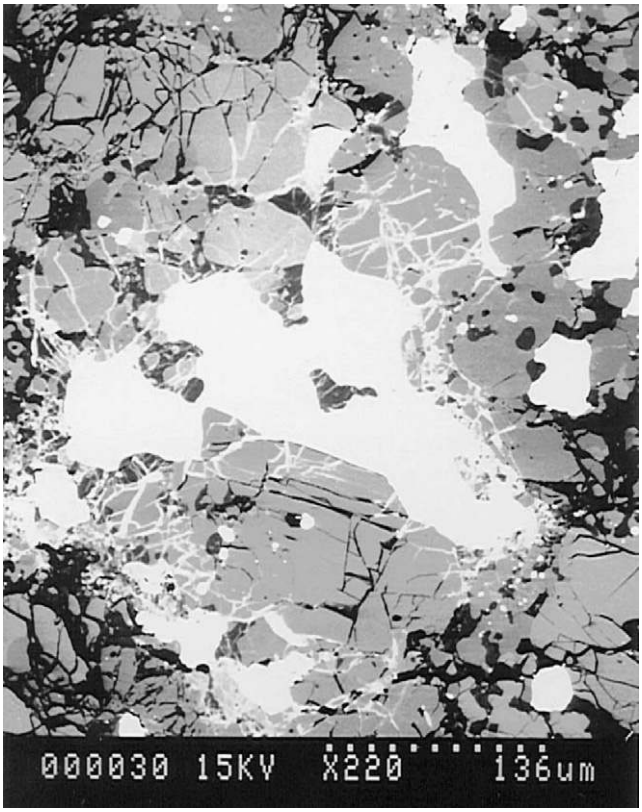

Fig. 4. The H5 ordinary chondrite Épinal in an SEM backscatter image. The large white areas are Fe, Ni grains; the dark lines are a series of microcracks, which account for the measured porosity. Note the microcracks partially filled with white material; this is interpreted as the oxidation product of terrestrial oxygen reacting with the meteoritic iron.

to be systematically higher than hand-sample porosities for the same sample. This is not seen in the data. Second, inspection of Fig. 4 shows that many of the cracks in contact with Fe/Ni metal grains (visible as large white areas) are themselves filled with high-density (white) material. Microprobe analysis of this material reveals the presence of Fe and Cl, but not Ni. We observe that microcracks in ordinary chondrite finds are consistently filled with such material, while it is absent in fresh falls. This material is clearly the result of terrestrial weathering, as water and chlorine enter through the microcracks and attack the Fe/Ni; the Cl promotes the oxidation of the Fe, but not the Ni. This weathering occurred over the many years that the sample sat in Earth's atmosphere. Épinal, the meteorite shown in Fig. 4, fell in 1822; this thin section was made at the Natural History Museum, London, in 1998, when this image was taken. Since the weathering occurred before the thin section was made, by inference the cracks filled with this weathering must also have existed before the thin section was made.

If the porosity of ordinary chondrites is indeed primarily the result of passing shock waves, then it is no surprise that all these meteorites have essentially the same porosity regardless of class, petrographic grade, or shock state. The impacts that produced these shock waves are a function only of the flux of available impactors; all bodies in a given region of the asteroid belt have presumably encountered a similar flux of impactors and thus should have similar porosities. The porosity in such a sample would be entirely produced after the chemical and metamorphic characteristics of the sample had been set: in essence, the porosity of the sample depends solely on the last time that its parent body had been hit by an impactor and experienced a shock wave.

However, the other corollary to this explanation is that the ground mass within the meteorite itself is essentially pore-free. This speaks to a greater question of importance to our understanding of the physical processes that occurred in the early solar system: what lithified the dust of the solar nebula into solid, rocky meteorites? Note that this is a very different question from the lithification of breccias. Breccias consist of pre-existing rock fragments held together by shock melting (cf. Bischoff et al., 1983); but ultimately, where did those rock fragments themselves come from? How did an accumulation of solar nebula dust, which models suggest should have been 80% or more porous (Blum et al., 2006), become ground mass with essentially zero porosity? Whatever lithified that dust succeeded in removing essentially all the porosity in the fine-grained ground mass, without melting the ground mass material. Note that shock compression produces heat (hence the shock melting in breccias), and the more the compression, the greater the heat. A single shock event compressing the dust directly into pore-free rock should release sufficient heat to completely melt the sample (Bowden, 2002), which clearly did not happen to these samples.

By contrast, the point-counting porosity derived by Corrigan et al. (1997) for carbonaceous chondrites is often significantly different from that measured by He pycnometry and glass bead density measurements. Only for four of the 26 meteorites that they measured do they report porosities greater than 20%, and only two more have porosities between 10% and 20%; 14 of the remainder have porosities of 5% or less. In eight cases, hand sample porosities for the same meteorite (if not the same sample) are also available. However, four of them are the four cases where the point-counting method did find porosities of 20% or more, in agreement with the hand sample measurements. Both methods also agree on relatively low porosities for Leoville and Vigarano. However, for Orgueil (CI) and Murray (CM), the hand sample porosities are around 30% while the point-counting method finds 3–4% porosity. These low porosity point-counting results are confirmed by Strait (personal communication) for Orgueil and Nogoya (CM).

An earlier suggestion by Corrigan et al. (1997) that the 35% porosity measured in a hand sample of Orgueil was due to terrestrial weathering of that meteorite (terrestrial sulfide formation as shown by Gounelle and Zolensky (2001), which they suggest would tend to crack the sample) is weakened when seen in this context. There is no evidence that Murray or Nogoya have been subjected to the kind of weathering seen in some Orgueil samples. And in fact the sample of Orgueil that was measured (by us) for porosity did not show visible evidence of such weathering, and it had been kept in a stoppered jar for more than 100 years. Furthermore, the fresh fall Tagish Lake (C) meteorite has an equally high porosity deduced both from its trajectory during its fall (Brown et al., 2002) and from direct measurements of retrieved samples (Hildebrand et al., 2006). On the other hand, as noted above, the grain density of Orgueil measured by carbon tetrachloride is smaller than that measured by pycnometry, while the bulk density measured by immersion into water is significantly larger than that seen by the glass bead method.

The difference between point-counting and He/bead porosity measurements most likely indicates that the porosity in carbonaceous chondrites is found on a scale either too large or too small to be seen easily in thin section. Large voids would not always be recognized in a thin section, and these voids, if big enough, would be more likely to take up water very quickly during bulk density measurements. Very small voids, too small to be visible in SEM images, would be more likely to be penetrated by He than carbon tetrachloride. Indeed, He could be penetrating between the molecular layers of the phyllosilicates found in CM and CI meteorites. Thus the water bulk density would be higher than the bead bulk densities, and the carbon tetrachloride grain density would be lower than the He grain density; indeed carbon tetrachloride and water would probably penetrate the same pore space yielding a porosity close to zero. These are in fact the trends seen in the data.

The opposite problem can be seen in several grain density and porosity measurements of basaltic achondrites. Model grain densities for several meteorites are significantly larger than the measured grain densities. One very likely explanation is that in these meteorites, a significant fraction of the porosity may be due not only to a well-connected network of microcracks but also to vesicles within the basalt. The diffusion rate of He through basaltic minerals is sufficiently slow (Lippolt and Weigel, 1988; Trull et al., 1991) that if these vesicles were not penetrated by any microcracks, they would not be found and filled by He during the pycnometry. This could explain the relatively low grain densities measured by pycnometry compared to the calculated model densities. If this is so, then it means that the microcrack porosity of the basaltic achondrites (which reflects their impact environment) is the measured porosity, not the model porosity.

3.3. Density and magnetic susceptibility as a classification technique

One useful side benefit to the measure of meteorite density is that it can provide part of a rapid, non-destructive system for classifying meteorite samples. Grain density is an intensive variable that varies with iron content and oxidation state, the same quantities that are used to characterize many different meteorite classes. Different classes of ordinary chondrites have distinctive ranges of grain densities, but with overlaps: H chondrites are distinctly more dense than L or LL chondrites, but the latter two groups do have significant overlap.

Another way to characterize a meteorite's iron content is by studying its magnetic properties. Magnetic susceptibility is the ratio of the induced magnetization of a material to the strength of an applied magnetic field (<1 mT); it depends on the capacity of the material to be affected by, or respond to, such a field and is a function of the abundance of the various magnetic phases in the sample, weighed by their specific susceptibility. The measurement of magnetic susceptibility is quick and non-destructive. Rochette et al. (2003) demonstrated that the magnetic susceptibility of unweathered ordinary chondrite falls is correlated with the amount and oxidation state of the iron within those meteorites, and that the L and LL classes are clearly distinguished by their magnetic susceptibilities. In their data, however, a small overlap occurs between H and L classes.

Terho et al. (1991, 1993) first suggested that correlating magnetic susceptibility with density could be a powerful way of resolving these ambiguities. However, they did not account for the effect of terrestrial weathering, which significantly lowers the grain density of finds versus falls while also lowering their magnetic susceptibility. For example, as weathering proceeds, the susceptibility and grain density of an H chondrite would eventually be lowered into the range of L chondrites. This makes the classification of finds by this method problematic.

However, this method is quite robust for fresh falls (Consolmagno et al., 2006a). The correlation between grain density, magnetic susceptibility, and meteorite type in our data set shows the overlap in *density* between L and LL, and a small overlap in *susceptibility* between the H and L meteorites, but by using both susceptibility and grain density together these ambiguities are resolved (Fig. 5).

Likewise, this method can be applied (Rochette et al., 2008) to carbonaceous and enstatite chondrites (Fig. 6).

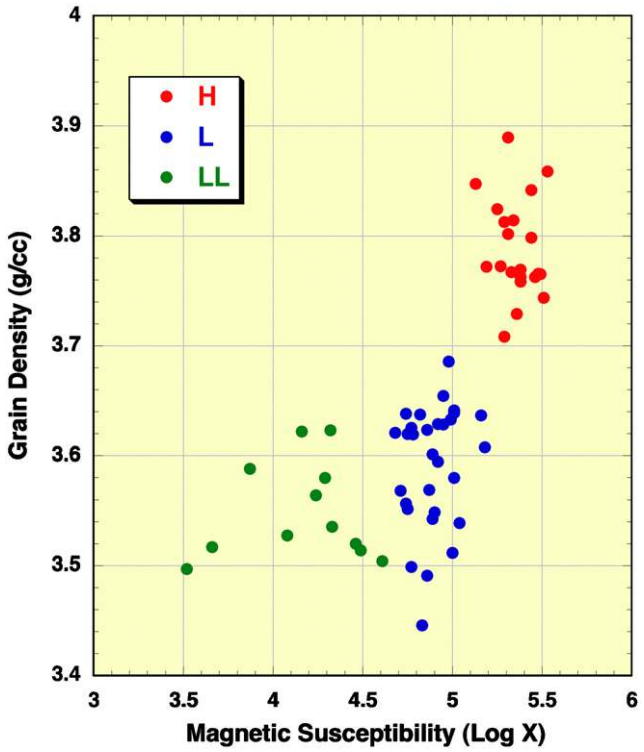

Fig. 5. Grain density and magnetic susceptibility for ordinary chondrites (fresh falls). Note that the combination of these two intrinsic factors cleanly groups the meteorite types into distinct regions of the plot. (In fact, the LL meteorite closest to the boundary between the L and LL group is Knyahinya, already labeled L/LL on chemical grounds.) Figure adapted from Consolmagno et al. (2006a).

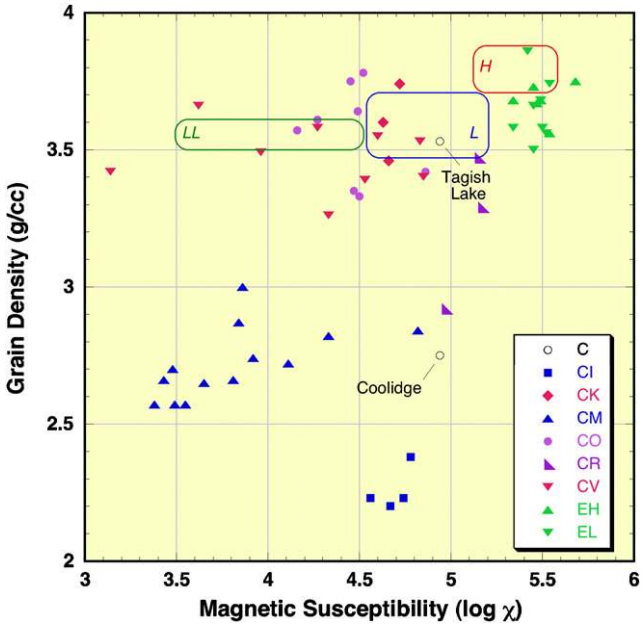

Fig. 6. Grain density and magnetic susceptibility for the C and E chondrites also defines clear boundaries, although with some overlap. Regions covered by H, L and LL chondrites are indicated by red, blue, and green outlines, (respectively). Figure adapted from Rochette et al. (2008).

The technique works in general to differentiate among certain classes of the carbonaceous meteorites, though there is an overlap between the related CV/CK classes and the CO class. Unfortunately, many of the C and E types also overlap the ordinary chondrite classes, however, limiting somewhat the ability of density and susceptibility alone to differentiate among stony meteorite classes.

Unlike traditional chemical tests, the measurement of physical properties is fast and non-destructive, and it characterizes the whole rock, making it especially appropriate for surveying large collections and in detecting misidentified samples (Rochette et al., 2003).

3.4. Science issues in asteroid/meteorite studies

This variation in porosity between major meteorite groups directly addresses issues of the formation of these bodies, and their parent bodies, in the solar nebula. If each meteorite's compositional type was formed in its own distinct area of nebular space, then this should also show up as significant differences in their physical states, beyond the obvious differences in chemistry and mineralogy. Different nebular conditions may lead to differences in accretional timing, accretional energy, lithification, and compaction, resulting in differences in microporosity. From our data, we conclude that the ordinary chondrites (and, albeit with less data, the other meteorite classes as well) are significantly more compacted and more completely lithified than most carbonaceous chondrites. Any hypothesis for the lithification of meteorites must account for this difference. In addition, the high porosity of some carbonaceous chondrites may be indicative of a lower overall crushing strength. As well as giving us an important clues to the structure of their putative parent bodies (the dark asteroids) this would have a direct effect on their survivability in atmospheric entry, suggesting that they are under-represented in our collections compared to their abundance in the solar system.

Another factor to look for is variation within meteorite groups. Porosity measurements are snapshots on the scale of a few centimeters of an individual sample's structure, but meteorite physical properties could vary over tens of centimeters or even meter scales. What degree of uniformity does formation within a zone of the solar nebula or residence in a particular region of the solar system impose on a meteorite type? How large is the range of variation in density, porosity and strength within the cosmochemical formation zone or region of the asteroid belt for a given mineral assemblage?

By measuring a statistically significant number of samples of ordinary chondrites in every metamorphic and shock grade, we have been able to characterize the variation within each meteorite groups' parent body as

being remarkably small; but if the L chondrites are indeed less porous than the H and LL groups, this might suggest that their parent body experienced a slightly different impact environment. We are a long way from completing a statistically significant sample of most other meteorite types. However, we have seen that the difference between reduced and oxidized CVs follows a pattern consistent with parent body modification of the reduced CVs (MacPherson and Krot, 2002).

A related measurement is to characterize the variation with a large single object. Falls such as Farmington and Pultusk are major showers of fragments, with hundreds of kilograms of individual stones that can provide insight into the range of physical variation in meteorites and the physical properties of their asteroidal parent bodies. Systematically measuring the porosity and density of these large falls characterizes any larger scale variations that may be significant in parent asteroids. Consolmagno and Britt (1998) earlier reported that significant porosity differences could be found from sample to sample in three of ten cases where multiple pieces of the same meteorite were measured. However, more extensive measurements of many samples, most of them whole rocks, from five large showers have not shown any significant variation in porosity from sample to sample (Consolmagno et al., 2006a; Macke, 2007). It may be that such variations are real but rare. This work needs to be extended to more examples of meteorite showers.

A related question is porosity variations in the different sized pieces of meteorites. Differences in porosity with the "scale" of the object would have a direct bearing on how meteorites lithify and also how they break apart upon atmospheric entry (Flynn et al., 1999). However, we have found that for ordinary chondrites there is no correlation with either the value or the spread of porosities for samples ranging in size from a few grams to several tens of kilograms (Fig. 1), and the success of the point-counting method in reproducing hand-sample porosity means that this uniformity extends down to the scale of a meteorite thin section. More data on other meteorite types can show whether this generalization can be extended beyond the ordinary chondrite case.

Meteorite porosity and density can provide insight into how asteroid materials respond to regolith-forming and shock processes. Are the meteoritic breccias, especially the regolith breccias, more or less porous than normal meteorites? Breccias are fragmental collections of shattered rock that have been re-lithified by shock, usually by grain-boundary melting under high pressures (e.g., Bischoff et al., 1983). There was a hint in our earlier data for ordinary chondrites (Consolmagno et al., 1998) that relithified breccias might be slightly less porous than the average for their groups. Now, given a larger database, we find only a marginal difference, less than 1% porosity, between breccias and non-breccias: the average model porosity of 61 ordinary chondrite breccias in our sample is $8.2 \pm 5.6\%$, while that for the non-breccia group is $9.0 \pm 4.7\%$.

Part of the issue of how asteroid materials respond to regolith processes is to determine the relationship between meteorite shock state and porosity. As seen in Fig. 3, we found fewer high porosity meteorites in shock state two compared to shock state one, and fewer again in shock state three; beyond that, however, increasing shock appears to have no influence on porosity. Note that we have only eight shock state five or six samples, however; and indeed, our conclusion for the lower shock states is based on only 11 high porosity ($>15\%$) samples in our dataset: Acfer 046, 073, and 098; Ambapur-Nagla; Allegan; Beaver Creek; Bjurböle; Forest Vale; Kiffa; Menow; and Saratov. None of these meteorites have been inspected by SEM for the location of their porosity. Inhomogeneities may play a role: many of these high porosity samples are notable for being unusually friable, but we have noticed that larger pieces (>145 g) of Allegan are much less friable than smaller pieces. And while measurements of 20 samples of Bjorböle ranging from 4 to 80 g by the Finnish group, and a 10 g piece by Flynn and Klock (1998), give high porosities, another measure by Wilkison et al. (2003) of a 142 g piece yields essentially zero porosity. This runs contrary to the general trend noted above that porosity does not depend on sample size.

The final stage in meteorite evolution is its processing after accretion to the Earth. Terrestrial weathering in ordinary chondrites increases the content of low-density clay minerals and iron oxides (Bland et al., 1996, 1998) and may result in the formation of carbonates in CO meteorites, filling void spaces and so lowering grain densities. However, we have seen no difference in grain densities between falls and finds among enstatite chondrites or CV/CK samples; how do they weather? Furthermore, the mechanism of weathering in Antarctic meteorites is distinctly different. Antarctic meteorite grain densities are, on average, comparable to those for falls, not finds. However, almost a quarter of the Antarctic meteorites (six of 27) in our database have unusually low bulk densities, and thus model porosities that are remarkably high, ranging from 20% to 33%. (ALH-77254, the only one of these measured for shock, is 20.4% porous but shock state 4!) Perhaps this high porosity is the result of freeze–thaw cycles within the meteorite during its stay on the Antarctic ice.

4. Meteorite porosity and the stratigraphy of the solar nebula

4.1. The meteorite–asteroid connection

The compositional diversity of the various types of meteorites spans a huge range, essentially from dirt

clods to steel, showing bulk densities that range from 1.6 to 7.8 g/cm^3.

But as diverse and interesting the meteorite collections are, the range of compositions observed in asteroids and comets is even larger. The high-density end seems fixed by iron–nickel combinations; observations do show asteroids with spectra consistent with Fe–Ni meteorites and this is backed up by radar reflectivity measurements consistent with metallic surface material. But the low end is nothing short of amazing. The bulk densities of comet nuclei lie in the neighborhood 0.5 g/cm^3 (cf. A'Hearn et al., 2005; Davidsson and Gutiérrez, 2006; Stansberry et al., 2006), substantially smaller than the densities of any of the major constituents of comets such as water-ice (0.93 g/cm^3), organic-rich silicate dust (~2.25 g/cm^3), or even methane ice (0.9 g/cm^3).

Since the 1970s efforts have been ongoing to classify the asteroids by their spectral colors (see Bus et al., 2002). At first, this classification was based only on broad visible colors and albedo (brightness). On that basis, asteroids with relatively high albedos that tended to be brighter in red filters were assigned to the S class; C class asteroids were dark and colorless; M asteroids, relatively bright but colorless. As technology advanced, allowing more detailed spectra extending into the infrared (where the characteristic bands of water and certain minerals are found), these groups have been further subdivided into an alphabet soup of different asteroid types. Some ambiguities in interpretation have been found; for example, a few examples of the putative metal-rich (M) asteroids have also been seen in the infrared to contain water bands, while others have been shown by radar reflection properties to indeed be rich in metal. Clearly the asteroids are more complex than the original S, C, M classification suggested. Nonetheless, this general attempt to connect asteroid spectral types with meteorite samples continues to be the basis of our classification.

There is strong evidence from the trajectories of recovered falls that most meteorites originated in the main asteroid belt, thus sampling the mineralogy and small-scale structure of at least some asteroids (Morbidelli and Froeschlé, 2003). However, there is also strong evidence that this is a biased and limited sample of the diversity in the asteroid belt. The evidence from detailed asteroid spectra now indicates that only a small fraction of asteroids contribute most of the recovered meteorites: although ordinary chondritic meteorites account for ~74% of meteorite falls, their putative spectral analogs, the S(IV)-subclass and Q-class asteroids, make up only a small fraction of the identified asteroids (Gaffey et al., 1993, 2002). Even the more broadly defined S-class, which may include compositional types similar to primitive achondrites, lodranites, brachinites, pallasites, and several other rare meteorite types as well as the ordinary chondrites, accounts for only ~17% of typed asteroids (Bus and Binzel, 2002; Rivkin et al., 2004) while their meteorite analogs contribute 85% of observed falls.

The relative physical strength of meteorites is probably the major biasing factor. Medium strength materials, such as stones, are probably vastly over-represented because they are weak enough in tension that they can be broken off and ejected from a larger parent body in the first place, but strong enough to remain coherent on ejection, and tough enough to get through the atmosphere. Very strong materials such as irons and stony-irons may be under-represented because of the difficulty in fragmenting and ejecting them from their parent bodies; very weak materials would not survive the trip from parent body to Earth's surface intact.

Indeed, the Earth's atmosphere is a potent filter. Atmospheric entry decelerates an object from its solar orbital velocity of 20–80 km/s (as observed in meteors hitting the upper atmosphere; cf. Hunt et al., 2003) to an atmospheric terminal velocity of a few hundred meters/second. Although most of that deceleration is taken up in friction heating, which can easily reach 1500 °C on the meteorite's surface and which vaporizes approximately 40% of a meteorite, it is quite common for larger meteorites to fragment during atmospheric entry, producing a "shower" of related meteorites that are then scattered by winds. The stress of impact onto the Earth's surface is the final direct stress.

While relatively strong meteorites (irons, stony-irons, ordinary and enstatite chondrites, achondrites, and many carbonaceous chondrites with substantial cohesive strength, primarily because of their high metal contents and strong igneous or metamorphic structure) make up over 95% of recovered meteorites, dark and volatile-rich materials from the outer asteroid belt, comets, or TNOs are rare. It is likely that any meteoroids from these objects would themselves be highly porous, composed of silicates mixed with organics, carbon compounds, and frozen volatiles. Such a mixture would have all the strength properties of a soggy dirt clod. This kind of material stands little chance of surviving the stress and heating of atmospheric entry; but there are exceptions, such as Orgueil and Tagish Lake. These meteorites are very weak, friable, porous, and volatile-rich and can be easily crushed by any moderate stress. In the case of Tagish Lake, only the unusual circumstance of its landing onto soft snow (in northern Canada during the month of January) allowed intact samples to be recovered; those fragments landing instead on nearby hard ice left no coherent samples, only large black splotches (Hildebrand et al., 2006).

Another factor adding to this filter against volatile-rich meteorites is that objects reaching Earth from the outer asteroid belt or cometary source regions will have much greater orbital velocities than those coming from

the inner asteroid belt, because of the larger potential energy of their orbits. Since the energy of the orbit and the stress of atmospheric entry scales by the square of velocity, the relatively weak and friable outer asteroid belt material tends to be subjected to much greater stresses than the relatively strong inner asteroid belt S-class materials.

Location and orbital dynamics within the asteroid belt also play a major biasing role. The dynamical processes most capable of perturbing asteroids, and thus meteorites, out of stable orbits in the main belt are resonances which operate in relatively narrow zones. Orbital resonances with Jupiter or secular resonances with Saturn greatly increase the eccentricies of the asteroids orbiting there, which increases the probably of collision and disruption. An asteroid will remain in such a zone for only a few million years before being perturbed into an orbit colliding with the Sun or a planet, or being ejected from the solar system. The vast majority of Earth-crossing asteroids appear to originate from just two such resonances in the main belt, the 1:3 Kirkwood Gap and the ν_6 resonance (Morbidelli et al., 2002; Morbidelli and Froeschlé, 2003). Both zones are in the inner asteroid belt where the asteroid population is dominated by S-type asteroids. Note that while these resonances perturb asteroids into planet-crossing orbits, the net result is usually not collisions with terrestrial planets. For example, numerical integrations of the activity of objects in the 1:3 Kirwood Gap showed that 70% impact the Sun, 28% are ejected from the solar system on hyperbolic orbits by Jupiter, and just 2% interact with the terrestrial planets (Gladman et al., 1997). Resonances in the outer asteroid belt are even less likely to perturb asteroids into the planet-cross population; material there is much more likely to be ejected by Jupiter. This is the way that the Oort cloud of comets was originally populated, and the process continues today with outer asteroid belt resonances.

Thus it is not surprising that the major source of our meteorites are relatively strong iron-rich stony asteroids in the inner asteroid belt, closest to Earth and in a region where several dynamical pathways can perturb asteroids into planet-crossing orbits.

4.2. Asteroid density

Knowledge of meteorite microporosity, grain density, and bulk density can be used to estimate the bulk porosity of asteroids and assess their internal structure. The starting points are the three pieces of data we can obtain about an individual asteroid: (1) its bulk density, (2) its reflectance spectrum, to indicate a meteoritic compositional analog, and (3) the grain density and average porosity of that analog meteorite. Recall that meteorite grain density is a density of an idealized completely solid, zero porosity object. Any deviation of the asteroid's bulk density from its meteorite analog's grain density provides an estimate the bulk porosity of the asteroid. That bulk porosity can in turn be divided into two components: the microporosity of the asteroidal material, which one can assume is the same as the porosity of the analog meteorite, and the macroporosity of large-scale voids within the asteroid itself.

Thus the first step in this process is to determine the density of an asteroid. Like any bulk density measurement, asteroid bulk density requires determination of mass and volume. The major problem is that both mass and volume determinations are challenging measurements to obtain remotely for small solar system bodies.

There are four robust methods for asteroidal mass determination: (1) asteroid–spacecraft perturbations; (2) asteroid–asteroid perturbations; (3) asteroid–planet perturbations; and (4) observations of the motion of asteroid satellites.

The first method, spacecraft–asteroid perturbations, can be by far the most accurate way to determine asteroid mass, but it is also one of the rarest, requiring an expensive spacecraft mission having a close encounter with the small body. The line-of-sight component of any asteroid-induced velocity change is determined by Doppler tracking data during a close encounter (e.g. Yeomans et al., 1997). The orbital solution for the spacecraft's motion provides the asteroid mass as one of the parameters that affect spacecraft trajectory. The accuracy of the solution improves with larger asteroid mass, closer approach distances, and longer periods in close approach. Orbiting the asteroid provides refinements such as gravity field and mass distribution as well as the total mass value, as shown in operations around 433 Eros (Yeomans et al., 2000). Under ideal circumstances of long orbital operations, mass determination errors can be a few tenths of percent.

The second method, tracking the motions of asteroids that have gravitationally interacted with other asteroids, requires modeling the orbits of multiple asteroids over long periods of time and deriving the perturbing masses required for observed changes. As with spacecraft perturbations, the best results are obtained with larger masses, closer approaches, and longer observational baselines. The best data, not surprisingly, are for the largest asteroids 1 Ceres, 2 Pallas, and 4 Vesta; they contain 60% of the mass of the asteroid belt, and they have an observational baseline over two centuries long. Errors for this method can be as low as a few percent; for smaller asteroids with short observational baselines errors climb rapidly.

For the third method, we note that the large asteroids Ceres, Pallas, and Vesta can produce perturbative amplitudes of more than 50 m per orbit on the motion of Mars. The position of Mars also has a long baseline of observations, and the precise location of Mars is

highly important for spacecraft operations; optical, radio, radar, and spacecraft data have located it to a precision of a few meters. Errors in the masses of these three largest asteroids via this method range between 0.3% and 9%, directly correlated with asteroid mass, and the inferred masses are in good agreement with the values found by the method previously described. More intriguingly, however, other, smaller asteroids also have non-negligible effects upon the orbit of Mars. Even though the perturbations of any particular small asteroid are not significantly larger than the observational accuracy of the Martian orbit determination, Standish (2001) (see also Standish and Fienga, 2002) modeled the mass of a few hundred of the largest asteroids by accumulating the perturbations of the asteroids as a group. He separated the perturbations by asteroid spectral class (noting that the S- and M-class asteroids predominate in the inner asteroid belt and the C types in the outer asteroid belt) and, with a few assumptions, solved for the mean bulk density of the spectral classes as a whole. These data confirm trends seen independently in the other bulk density data: the C class average as $1.4 \pm 0.05\,g/cm^3$, the rocky S class as $2.69 \pm 0.04\,g/cm^3$, and the metal-rich M-class averages $4.7 \pm 0.5\,g/cm^3$ (Standish, 2001).

The fourth and by far the most productive method of asteroidal mass determinations is the observation of asteroidal satellites. Once an asteroid's satellite has been discovered, this method can provide a very accurate mass for that asteroid since, by Kepler's third law, the orbital period and semi-major axis of the satellite will uniquely determine the mass of the primary. The best observations yield errors of only a few percent in mass (Merline et al., 2002). The challenge is, first, to find an asteroid with a satellite; and then, once you have caught your satellite, to observe it long enough to determine its orbit accurately. This can be quite difficult. Direct optical observation of asteroidal satellites requires the use of adaptive optics instrumentation on the largest telescopes and observational time is extremely limited. A major challenge is to have enough observations to overcome ambiguities in the plane-of-the-sky satellite orbital parameters and any obscuring effects of glare from the primary. An extremely productive alternative to optical imaging is the use of Goldstone and Arecibo radar tracking to characterize satellite orbits (Nolan et al., 2001; Margot et al., 2002; Ostro et al., 2002). Again, the critical factor in error reduction is sufficient observational time to characterize the satellite orbit with confidence. Another method uses asteroid "lightcurves" to eliminate the need for huge instrumentation. If a satellite's orbital plane overlaps the line-of-sight position of the primary, then the satellite will partially eclipse, and be eclipsed by, the primary. This will cause a periodic change in the amount of light reflected by the asteroid–satellite system, which can be observed even with very modest (0.5–1 m) telescopes. All that is required is a long baseline (on the order of 80 h) of measurements of the asteroids' brightness. Analysis of the changes to that brightness pattern will yield solutions for the satellite's orbital period and semi-major axis, from which an asteroid mass can be computed.

Once an asteroid's mass has been determined, the next step in estimating an asteroid's bulk density is to determine the asteroid volume. Ironically, while finding any mass at all for an asteroid is the most problematic part of finding its density, once that mass has been determined the major source of uncertainty in determining an accurate density is generally the volume determination. The problem arises because volume is 3-D, while any given asteroid observation (ground based or spacecraft) is a "plane-of-the-sky" two-dimensional snapshot of an often partially illuminated, highly irregularly shaped non-spherical object. The best situation is a spacecraft orbital mission that can repeatedly view all aspects of an asteroid using optical and laser-ranging instruments to build up a 3-D model of the asteroid's shape. This was done for the NEAR mission to 433 Eros, and the resulting shape model had volume errors of a few percent (Yeomans et al., 2000). More typical for spacecraft encounters are fast flybys, however, where whole hemispheres are not imaged at all because small body rotation is typically slow relative to the time period that the body is resolved by the spacecraft. The resulting volume errors are on the order of 12–15%.

Remote methods for volume determination can use imaging, radar, and infrared flux observations. Hubble images and adaptive optics using the largest telescopes have produced relatively detailed imaging and shapes for a few of the largest asteroids (Ceres, Vesta, Pallas). These, combined with stellar occultations which give direct measurements of plane-of-the-sky cords across the body of the asteroid, have produced low-error (~5%) volume estimations of these asteroids. Radar imaging (cf. Nolan et al., 2001; Margot et al., 2002; Ostro et al., 2002) is probably the best remote method where resolutions of a few hundred pixels across the surface of a small body can produce detailed shapes with imaging over full rotation periods. This technique is useful for a number of objects including some very small near-Earth asteroids, but is primarily limited by the distance of the target asteroid. For close-approaching asteroids, radar imaging can yield very accurate volume estimates with errors on the order of the best large asteroid observations. The most common method for determining asteroid volume, however, is the use of the asteroid diameter data from the Infrared Astronomical Satellite (IRAS) Minor Planet Survey (Tedesco et al., 1992). The IRAS observations at two wavelengths in the plane-of-the-sky give an effective area from which the

flux is being emitted; from this area, major and minor axis radii and thus a volume can be estimated. This is, of course, a simplified model based on a two-dimensional snapshot of a complex 3-D shape. Errors for this method vary not only with the number of measurements and the quality of data but also with how closely the highly irregular shape of the asteroid can be approximated by a triaxial ellipsoid. The uncertainties in volume probably range between 15% and 20%, and thus account for the majority of the uncertainty in asteroid bulk density estimates.

4.3. Meteorite density and asteroid structure

Given an asteroid's bulk density, we can then proceed to derive insights into the asteroid's internal structure. One can extract an estimate of the asteroid's large-scale porosity, or *macroporosity*, by comparing the asteroid's bulk density with a typical meteorite analog bulk density. Macroporosity represents void spaces whose dimensions are on the order of the dimensions of the meteorites themselves, or larger (as opposed to the microporosity measured within the meteorites themselves). While such macroporosity has never been directly imaged, the parallel grooves seen in images of Phobos and the body-wide faults of Eros give us some hints as to the way this macroporosity could be expressed within an asteroid. The pore spaces could be in the form of widespread cracks, centimeters to meters wide, that could extend through the entire length of the asteroid.

Estimates of the macroporosity of those asteroids for which densities have been estimated are shown in Table 6 and Fig. 7. Four clear trends are visible in this figure. First, the largest asteroids (with masses greater than 10^{20} kg) all have essentially zero macroporosity. Perhaps bodies of this size or larger were sufficiently large that they never suffered catastrophic disruptions and reaccretions; or perhaps they have sufficient gravity to remove macroporosity from their interiors. This has a significant implication for our definition of the boundary between "dwarf planets" and small solar system objects like comets and asteroids, as even a small icy body of 500 km radius or so apparently is sufficiently large enough to pull itself into a shape controlled by an equilibrium between gravity and spin. More than a dozen such objects have already been discovered in the trans-Neptunian population. Second, by contrast, virtually all asteroids smaller than that mass have at least 20% or more macroporosity. The NEAR team have attributed Eros' ~20% macroporosity to extensive internal cracking of an otherwise coherent body (Wilkison et al., 2002) but more macroporous bodies, like Itokawa (imaged by the Hayabusa spacecraft), could be "rubble piles" resulting from catastrophic disruption and reaccretion (Melosh and Ryan, 1997; Wilson et al., 1999). Third, although there are exceptions in both cases, we note that in general the roughly 20% macroporous bodies tend to be S-type asteroids, while the much more macroporous bodies tend to be C types. Finally, the icy bodies of the outer solar system – comets, centaurs, and TNOs – are all extremely macroporous. We also note that the M-class asteroid 16 Psyche must be very porous if it is in fact metallic. The identification of many M asteroids as irons is controversial; for example, Margot and Brown (2003) have argued that the M asteroid 22 Kalliope is in fact more like a chondrite.

Note that our estimate of small body macroporosity requires two assumptions. First, do we know the asteroid's meteorite analog? In many cases it is difficult to determine precise asteroidal mineralogy, and the mineralogy of a given asteroid may not actually be represented in the meteorite collection. However, most meteorites that are likely analogs for the S class asteroids have very similar bulk densities; our results are not strongly sensitive to the actual meteorite analog chosen for a given asteroid. In the calculation here, we use the average bulk density of an L chondrite. For the C and related dark asteroids, the problem is trickier. The lowest density meteorites, the CI class, are not well characterized (only Orgueil, and the unusual Tagish Lake meteorite, have low bulk densities measured) and they are both very porous and very easily crushed, which raises the question of whether their low density is a reasonable representation of the density of material inside a moderately sized asteroid. In addition, they have high water contents (~20%), whereas many of the dark bodies, including Mathilde and Phobos, do not have the characteristic absorption band of OH in their spectra (Rivkin et al., 1997, 1999). We use the bulk density of CM meteorites as a more likely analog for dark, organic-rich material.

Second, are these meteorites still representative of that asteroid's material even after they have been ejected from their parent bodies and delivered to Earth? By using bulk rather than grain densities for the meteorite analog, we are in effect subtracting the average meteorite analog's microporosity from the total porosity of the asteroid. This assumes that the microporosity of the meteorites today was already present when the material was still emplaced in its parent body. Given our discussion of the nature and origin of meteorite porosity, we have confidence in this assumption, especially for the well-studied ordinary chondrites and their S-asteroid counterparts. For that case, we found that the porosity is uniform across all types and metamorphic histories, and we deduced that it is due almost entirely to post-formation shocks. Given the collision environment of the inner asteroid belt, and the evidence of extensive cratering on the surfaces of these asteroids,

Table 6. Asteroid bulk densities and macroporosities

Object	Density (g/cm^3)	±	Mass (kg)	*a* (AU)	Asteroid class	Meteorite analog	Macro-porosity (%)	± (%)	Ref.
1 Ceres	2.12	0.04	9.45×10^{20}	2.77	C	Dusty ice	0.0	2.5	1
2 Pallas	2.71	0.11	2.15×10^{20}	2.77	C	CM	0.0	4.9	1
4 Vesta	3.44	0.12	2.74×10^{20}	2.36	V	L Chon.	0.0	3.6	1
11 Parthenope	2.72	0.12	5.13×10^{18}	2.45	S	L Chon.	19.0	3.6	2
16 Psyche	2.00	0.6	1.73×10^{19}	2.92	X/M	Iron	73.3	8.0	3
20 Massalia	3.26	0.6	5.25×10^{18}	2.41	S	L Chon.	3.0	17.9	4
22 Kalliope	2.03	0.16	7.36×10^{18}	2.91	X/M	L Chon.	39.6	4.8	5
45 Eugenia	1.12	0.3	5.80×10^{17}	2.72	C	CM	50.2	13.3	6
87 Sylvia	1.20	0.1	1.48×10^{19}	3.49	X/C	CM	46.6	4.4	6
90 Antiope	1.25	0.05	8.30×10^{17}	3.15	C	CM	44.4	2.2	7
107 Camilla	1.88	0.2	1.09×10^{19}	3.49	X/C	CO	38.0	6.6	6
121 Hermione	1.10	0.3	5.40×10^{18}	3.45	C	CM	51.1	13.3	6
243 Ida	2.70	0.4	4.20×10^{16}	2.86	S	L Chon.	19.6	11.9	8
253 Mathilde	1.30	0.2	1.03×10^{17}	2.65	C	CM	42.2	8.9	9
283 Emma	0.87	0.02	1.48×10^{18}	3.05	C?	CM	61.3	0.9	6
379 Huenna	1.16	0.13	4.77×10^{17}	3.14	C	CM	48.4	5.8	6
433 Eros	2.67	0.03	6.68×10^{15}	1.46	S	L Chon.	20.5	0.9	10
617 Patroclus	0.80	0.2/0.1	1.36×10^{18}	5.23	P	Dusty ice	51.8	12.0/6.0	11
762 Pulcova	1.80	0.8	2.70×10^{18}	3.16	F	CM	19.9	35.6	12
3671 Dionysus	1.60	0.9/0.4	2.00×10^{11}	2.20	C	CM	28.8	40/17.8	13
3749 Balam	1.20	0.6	1.50×10^{14}	2.24	S	L Chon.	64.3	17.9	6
5381 Sekhmet	1.98	0.65	1.05×10^{12}	0.95	V?	HEDs	34.0	21.7	14
25143 Itokawa	1.95	0.14	3.58×10^{10}	1.32	S	L Chon.	42.0	4.2	15
1998 SM165	0.52	0.29	6.78×10^{18}	47.41	TNO	Dusty ice	68.7	17.5	16
1991 VH	1.60	0.5	1.50×10^{12}	1.14	S	L Chon.	52.4	14.9	17
65489 Ceto	1.38	0.7/0.3	5.42×10^{18}	102.63	Centaur	Dusty ice	16.9	39.2/19.3	18
65803 Didymos	1.70	0.4	2.00×10^{11}	1.64	Xk	CM	24.4	17.8	13
1999 KW4	1.97	0.24	2.33×10^{12}	0.64	S	L Chon.	41.4	7.1	19
Pluto	1.92	0.12	1.31×10^{22}	39.48	TNO	Dusty ice	0.0	7.2	20
136199 Eris	2.30	0.3	1.66×10^{22}	67.73	TNO	Dusty ice	0.0	18.1	21
1996 FG3	1.40	0.3	2.10×10^{12}	1.05	C	CM	37.7	13.3	22
2000 DP107	1.70	1.1	4.60×10^{11}	1.37	C	CM	24.4	48.9	23
2003 EL61	3.00	0.4	4.20×10^{21}	43.34	TNO	Dusty ice	0.0	24.1	24
29P/Borrelly	0.24	0.06	1.50×10^{13}	3.59	Comet	Dusty ice	85.5	3.6	25
81P/Wild2	0.49	0.11	1.50×10^{12}	3.45	Comet	Dusty ice	70.5	6.6	26
9P/Tempel 1	0.40	0.6/0.2	4.50×10^{13}	3.12	Comet	Dusty ice	75.9	36.1/12.0	27
Average S	2.69	0.04			S	L Chon.	19.9	1.2	1
Average C	1.40	0.05			C	CM	37.7	2.2	1
Average M	4.7	0.5			M	Iron	40	13	1
Charon	1.63	0.07	1.52×10^{21}	39.48	TNO	Dusty ice	1.8	4.2	28
Deimos	1.34	0.83	1.36×10^{15}		C	CM	40.4	36.9	29
Phobos	1.53	0.1	8.80×10^{15}		C	CM	32.0	4.4	29
SL9 (pre 1990)	0.60	0.1	7.30×10^{13}		Comet	Dusty ice	63.9	6.0	30

References: 1: Standish (2001); 2: Viateau and Rapaport (1997); 3: Viateau (2000); 4: Bange (1998); 5: Margot and Brown (2003); 6: Marchis et al. (2005); 7: Descamps et al. (2007); 8: Petit et al. (1997); 9, 10: Yeomans et al. (1997, 2000); 11: Marchis et al. (2006); 12: Merline et al. (2002); 13: Pravec et al. (2006); 14: Neish et al. (2003); 15: Abe et al., 2006; 16: Spencer et al (2006); 17: Rabinowitz et al. (2005); 18: Grundy et al. (2006); 19: Ostro et al. (2006); 20: Buie et al. (2006); 21: Brown and Schaller (2007); 22: Mottola and Lahulla, 2000; 23: Margot et al. (2002); 24: Rabinowitz et al. (2006); 25, 26: Davidsson and Gutiérrez (2003, 2006); 27: Richardson et al. (2007); 28: Person et al. (2006); 29: Smith et al. (1995); 30: Asphaug and Benz (1996).

it is clear that they have continually suffered shock events. There is a wide range of shock states among different meteorites, even though all meteorites must have experienced the similar shock of ejection from a parent body and landing on Earth; obviously, the meteorites were exposed to a long series of shock events, of varying strengths, while still on their parent bodies. Thus, it is unlikely that the porosity of meteorites

resulted only from the shock event that ejected the samples from the parent bodies into Earth-crossing orbits (or, only from the shock of impact with the Earth's atmosphere and surface). At the very least, we would argue that the shock of ejection from a parent body and landing on Earth should not have produced microcracks that were in any way substantially different from microcracks already in place in the samples. Rather, we conclude that the final shock events in the transport of these meteorites to the Earth's surface merely redistributed microcracks already present from continual episodes of shocking on the parent body.

These assumptions are less secure for the darker C-type asteroids and their carbonaceous chondrite analogs. In Table 6 and Fig. 7 we used the lower bulk density of "wet" CM chondrites as our analog for these asteroids; a higher-density CO-like bulk density would result in even larger macroporosities than the already-large values for most C-type asteroids (though such an analog would not adequately reproduce their low albedoes). On the other hand, if low-density C asteroids are made of material like Orgueil and Tagish Lake, their macroporosities could drop to about 20–30%.

Another standard assumption in this estimation is that any asteroidal pore space is empty. If the pore spaces were filled with some material such as water-ice, the amount of pore space required to explain the low bulk density of the object would increase dramatically. In the case of a low-density object like 243 Mathilde with a bulk density of 1.3 g/cm^3, its bulk density is not significantly higher than water-ice (at 0.97 g/cm^3) and it would require huge (i.e. $>75\%$ by volume) components of water-ice to account for its low density given the grain density of its meteorite analog (Britt and Consolmagno, 2000; Britt et al., 2002).

What can be said about the mineralogy and density of comets? It is possible to estimate the grain density of a comet from the materials seen in the coma, and proportions estimated from models, but except for the dust particles returned by Stardust actual samples that unambiguously come from a comet are not available. No meteorite has been linked convincingly with a comet origin (Campins and Swindle, 1998; Swindle and Campins, 2004). Clearly some interplanetary dust particles (IDPs) have a cometary origin, but other IDPs come from asteroids, and it is not clear which among the wide range of IDPs best represents cometary material. Some trends are present in the IDP data: meteors with lower entry velocities are more likely to be hydrated and more likely to have higher bulk densities, and so presumably are more likely products of asteroids rather than comets. But these trends all have exceptions; there is no perfect correlation among entry velocity, density, and chemical composition (Joswiak et al., 2007). Future comet sample return missions may provide the missing data. Nonetheless. the densities of the meteorites do put limits on the likely range of materials to be found within comets, because they are materials made in the same solar nebula from the same cosmic abundances as the non-icy material in comets: they are a ground truth for what kind of chemical compositions (and physical structures) this solar system's nebula actually did produce. Using as a "best guess" that comets are roughly equal volumes water-ice and organic material with a CM-like density (since the rock is roughly twice as dense as the ice, this is a mass ratio of about 2:1 rock to ice) we can guess at a bulk density of about 1.6 g/cm^3 for the material likely to make up comets. (This density in fact matches the smallest well-measured icy dwarf planet, Pluto's moon Charon, which presumably is large enough to have zero macroporosity but small enough to avoid significant internal compression.) When the inferred density of comet nuclei are compared against this bulk density, as we have done in Fig. 7, one can only conclude that comet nuclei are extremely porous.

A number of other small body science questions related to density and porosity can be stated, though some are exceedingly difficult to address. For example, what is the nature of asteroid and comet surface material? Do asteroid spectra in the visible and near-infrared, controlled by the optically active top few microns of an asteroid, provide an accurate characterization of asteroidal material in general? By comparison, we know that the top of the Moon's surface is characterized by "fines" that are highly porous, 50% or more (Heiken et al., 1991). Some of its surface material consists of interconnected bits of dust in a very loose structure sometimes referred to as "fairy castle structure." Emery et al. (2006) proposed that a similar structure could occur on the surfaces of asteroids and comets. Modeling the infrared emission of dust from comets (Lisse et al., 1998) indicates that a large number of comet dust particles in space do have such a loose structure; but most IDPs captured in the stratosphere do not (Love et al., 1994). If even small IDP-sized particles of very low density are affected by the filter of the atmosphere, certainly meteorite-sized samples of such material would not survive the filter of passing through the terrestrial atmosphere at high speed.

One way to characterize the regolith of asteroids is to measure the amount of power dissipated in radar waves reflected off their surfaces. The power dissipated is directly related to the amount of material encountered by the radar wave, which penetrates to a depth comparable to the radar wavelength (tens of centimeter). By assuming a meteorite analog for a given type of asteroid, one can compare the measured grain density of the analog material with the inferred bulk density of the material encountered by the reflected radar wave, to deduce the porosity of the regolith soil. Regolith porosities for 36 main belt asteroids have been deduced by this method. They range from 25% to 75% (Magri

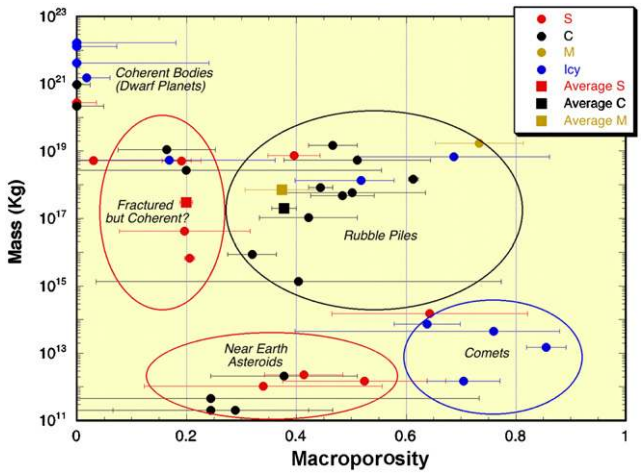

Fig. 7. Estimated macroporosity for a range of small bodies including main belt asteroids, TNOs, near-Earth asteroids, and comets. Asteroid macroporosity is estimated by subtracting the average porosity of asteroid's meteorite analog from its bulk porosity. Since microporosity probably does not seriously affect the structural integrity of small bodies, this is a direct estimate of the large-scale fractures and voids that determine the asteroid's internal structure. Only the largest objects with masses of over 10^{20} kg appear to be coherent and have low macroporosity, whereas small bodies have substantial macroporosity. Adapted from Britt et al. (2002).

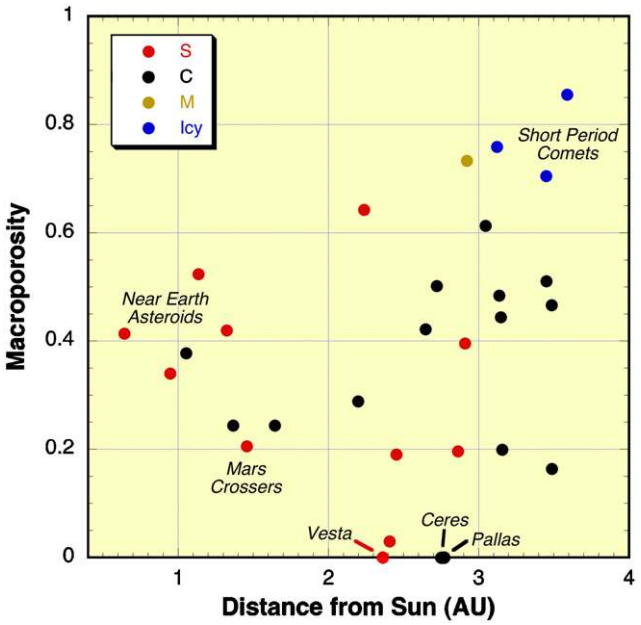

Fig. 8. Macroporosity of asteroids as a function of their location in the asteroid belt. Note the trend toward higher macroporosities at greater heliocentric distances. The S-type asteroids (red) tend to be found more in the inner belt, and the darker C-type bodies (black) further out, but there is significant overlap. Likewise, S asteroids in the main belt tend (with exceptions) to be have less macroporosity than the C asteroids, but this trend does not hold among the near-Earth population. Icy bodies and short-period comets, found in the outer belt, tend to be very macroporous.

et al., 2001). No correlation of regolith porosity with asteroid type or size is seen.

4.4. The stratigraphy of the solar nebula

In Fig. 8 we plot the macroporosities of the asteroids measured to date as a function of their position in the asteroid belt. Though there is significant mixing among the types and macroporosities, one can see there a trend of higher macroporosities to be found further out in the asteroid belt. An understanding of this compositional and density diversity in the asteroid belt and the rest of the solar system small body population, as revealed by comparison with their meteorite analogs, can be approached by treating small bodies as a series of zoned geologic units within a stratigraphic sequence starting at the inner edge of the main asteroid belt and working outward away from the Sun. These units have their origins in the unique temperature and geochemical conditions existing during condensation of the solar nebula and the initial accretion of planets.

The idea of a chemically zoned solar nebula controlled by proximity to the nascent Sun was first elaborated by Urey (1952) and Lewis (1974); for a review, see Barshay and Lewis (1976). An analysis of asteroid spectral classes vs. their orbital locations (Gradie and Tedesco, 1982; Cellino, 2000) shows just such a distinct gradation of material types within the asteroid belt as a function of distance from the sun: the high-to-moderate-temperature silicate minerals are observed to dominate the inner solar system at heliocentric distances of less than approximately 2.5 AU, while lower-temperature carbonaceous minerals are common in the cooler, outer regions of the solar system beyond 2.5 AU. This is an important boundary since apparently it marks the location where cooling temperatures allowed carbon compounds to form. At about 3.5 AU, the nebula was cool enough to allow the formation of water-ice. The transition between moderate and low-temperature nebular condensates is apparently what is seen in the zonation of the asteroid belt and the other small bodies.

Beyond this general trend, in fact, a more detailed compositional stratigraphy can be deduced from the spectra of small bodies in the solar system. The observation of asteroidal spectra groups shows, first, an innermost major group of small bodies peaking at about 2 AU; these are the E class asteroids whose meteorite analogs, the enstatite chondrites and achondrites, are composed of iron-free enstatite and unoxidized iron–nickel, indicating formation under high-temperature, relatively reducing conditions. So far, we have no data on the densities, or inferred macroporosities, of any E class asteroids.

The next major group out is the S class (along with the smaller V, A, R, K, and M classes), thought to be rich in the moderate-temperature silicates olivine and pyroxene, and both large amounts of free iron–nickel and iron oxides in the mineral phases, which indicate more oxidizing conditions. The mineralogy of these objects varies from almost pure olivine to almost pure pyroxene. With this wide range of mineralogies comes a wide range of meteorite analogs and possible formation scenarios whose common theme is varying degrees of post-accretional heating. The nebular geochemistry in this zone was apparently dominated by olivine and pyroxene chondrules with a strong admixture of Fe–Ni metal, but essentially no water. Included in the S class are undifferentiated but metamorphosed asteroids that are the parent bodies of ordinary chondrite meteorites. The typical macroporosity of S class asteroids ranges from 20% to 30%, though exceptions (both lower and higher) have been observed.

In addition to these familiar types there is also a range of asteroids that did melt and differentiate. The meteoritic/asteroidal materials include samples from what is apparently the core (iron meteorites and at least some M-class asteroids), the core-mantle boundary (pallasite meteorites), the mantle (brachinite meteorites?; A, S(I), S(II) class asteroids?), and the crust (HED – howardite, eucrite, and diogenite – meteorites; V class asteroids). Notably absent in our meteorite collection are samples that would come from the dunite-rich mantles of such differentiated asteroids yet can be directly connected via chemical trends to the abundant crustal basaltic meteorites; this has lent support to the idea that most crustal meteorites (the interrelated HED classes) come from a still-intact parent body (presumably Vesta or smaller asteroids chipped from Vesta). However, the presence of iron and stony-iron meteorites, and of rarer basaltic meteorites that cannot be easily connected to the HED classes, shows that other, no longer intact, differentiated parent bodies must have existed. The density of Vesta, and the chemistry of the HED meteorites, is consistent with an L-chondrite composition body that melted into a basaltic crust, dunite mantle, and iron core. This would be a differentiated body with zero macroporosity; in effect, a dwarf planet. Macroporosities exist for two M-class asteroids, but their identification as being metallic is not certain; if so, they would be extremely macroporous (on the order of 70%).

Another small asteroid class in this zone are the K asteroids, which have the CV and CO carbonaceous chondrites for meteorite analogs. They are metamorphosed, anhydrous carbonaceous chondrites low in carbon. Their presence here fits well into the pattern of higher temperature pre- and post-accretionary processing in this zone. As we have argued above, the grain densities of most of these meteorite types do not vary much from a value of about 3.5 g/cm^3. However, to date we do not have densities for any of these asteroids.

Peaking at around 3 AU are the dark asteroids of the B, C, F, and G classes whose meteorite analogs are the dark CI or CM carbonaceous chondrites. This area represents a major transition in small body mineralogy to less free metal, more oxidized silicates, important low-temperature carbon minerals, and significant amounts of volatiles such as water. The spectral differences between these classes are thought to represent varying histories of aqueous alteration or thermal metamorphism; the CI carbonaceous chondrites are rich in water, clay minerals, volatiles, and carbon and represent primitive material that has been mildly heated and altered by water. This zone starts the area where ices were stable during accretion and some ice was incorporated into these parent bodies; the post-accretionary heating was strong enough to melt at least some of the ices and produce the movement of aqueous fluids and the breakdown of some minerals into hydrated clays. The macroporosity of asteroids in this class tends to range from 30% to 60%.

The P asteroids peak at about 4 AU, and the D asteroids at 5.2 AU. Water of hydration (which is what is responsible for much of the low density of the CI and CM meteorites) is absent; this material was presumably too cold for any ice to have melted and reacted with the non-ice phases (Lebofsky et al., 1990). However, at this solar distance, frozen volatiles (mostly water-ice) would compose about one-third of mass with the rest being in the form of loosely packed, low-temperature materials such as carbon compounds, complex organics, fine-grained silicates, and water-ice. Thus their grain densities should be even lower than the 2.4–2.8 g/cm^3 of the CI and CM meteorites. Indeed, the spectral characteristics of these asteroids are difficult to duplicate with material that is delivered to the inner solar system. Delivery of meteorites from this zone is problematic because of the proximity of Jupiter, the existence of a number of resonance zones between the outer asteroid belt and the inner planets, and the distance involved. By far the most likely outcome for a perturbed P or D asteroid is gravitational interaction with Jupiter that ejects it into the Oort cloud, the home of long-period comets, and these ''asteroids'' may share characteristics with long-period comets, perturbed from the Oort cloud back into the inner solar system. What data we have on bulk density for objects in this zone (the Jupiter Trojan object 617 Patroclus, at 0.8 ± 0.2 g/cm^3 [Marchis et al., 2006]) do point to similarities with comets. Comparing that density against an inferred 1.5–2 g/cm^3 density for the solid matter of which is it made implies a 45–60% macroporosity in this region.

The final small body zone (sometimes referred to as the Kuiper Belt or Edgeworth-Kuiper Belt) is that of the TNOs. This is the source region for the short period

Jupiter-family comets. In many ways, studies of the TNOs today are at the same stage where asteroid studies were in the 1970s. Because of their faintness, spectra can be found for only the largest of objects; a more general classification must be based on broad-band colors. The first efforts have been made toward such a classification (Fulchignoni et al., 2003), and Tegler et al. (2003) have noted a possible relationship between TNO colors and orbital properties consistent with a primordial thermal gradient in the region where they were formed. However, it is clear that this region is not without its complexity. Among those objects large enough for spectra to have been taken (Roush et al., 1996; Brown et al., 2005; Licandro et al., 2006; Tegler et al., 2007, 2008), some of them such as Pluto, Eris, and dwarf planet 2005 FY9 show the strong absorption bands of methane ice while others, including Pluto's moon Charon and the dwarf planet 2003 EL61, do not. The reason for this difference is still not clear. Likewise, there are notable differences observed in color, albedo, and the presence or absence of binaries between TNOs in dynamically perturbed vs. unperturbed orbits (cf. Noll et al., 2007 and references therein).

Recent dynamical studies (Bottke et al., 2002; Levison and Morbidelli, 2003; Morbidelli et al., 2007) suggest that TNOs are the remnants of bodies that formed outward of the accreting gas-giant planets and were likely "pushed" into their present position in the so-called Kuiper belt by the outward migration of Saturn, Uranus and Neptune. As such, TNOs are currently about 8–10 AU farther out from the Sun than where they originally formed. Indeed, the TNOs are probably more primitive and low-temperature than the far more distant Oort cloud long-period comets; this is a case where the stratigraphy of the solar system was "inverted" by the action of Jupiter gravitationally perturbing nearby small bodies into the Oort cloud at the very edge of the solar system. (By conservation of angular momentum, this would also have moved Jupiter inwards toward the Sun, in the process allowing its resonances to sweep through the outer asteroid belt and efficiently depopulate that region.)

Given the location of their origin, these bodies should incorporate a range of exotic volatiles including nitrogen, methane, ethane, and CO_2 ices and clathrates, along with abundant water-ice. Spectral and broad-band color data indicate that at least some of the surfaces are rich in organic materials as well as water-ice and crystalline silicates. Like the Jupiter zone objects, these small bodies are probably composed of carbon compounds, complex organics, fine-grained silicates, and water-ice, with a larger proportion of exotic low-temperature volatiles although, as noted above, a wide variety of compositions can be expected from object to object. While the largest TNOs such as Pluto and Eris have bulk densities of $\sim 2.0\,g/cm^3$, many of the smaller TNOs share the extremely low densities of the comets (TNOs 47171 [1999 TC36] at $0.5 \pm 0.3\,g/cm^3$ [Stansberry et al., 2006]; 26308 [1998 SM165] at $0.52 \pm 0.29\,g/cm^3$ [Spencer et al., 2006]). Assuming an equilibrium between shape and spin rate, Tegler et al. (2005) proposed a density for Centaur 5145 Pholus at $0.5 \pm 0.2\,g/cm^3$, and Consolmagno et al. (2006b) argued on the basis of spin/shape statistics that TNOs in general should average a density near $0.5\,g/cm^3$. Lacerda and Jewitt (2007) have come to similar conclusions based on light curves for other TNOs. (Since even a small amount of internal strength can complicate the derivation of density from shape and rotation rate, these proposed density values are less robust than those tabulated in our Table 6.) Note, however, that Centaur 65489 Ceto/Phorcys, a close binary, has recently been shown to have an intermediate density of $1.37 + 0.66/-0.32\,g/cm^3$ (Grundy et al., 2007]). Given the "grain densities" of the ices and carbon-rich dust which make up these comets, their having bulk densities in this range means that they must have macroporosities of approximately 60–80%.

TNOs presumably do not contribute to the meteorite collection, but since they supply the Jupiter-family comets, samples of cosmic dust and the recent Stardust comet coma sampling mission shed light on some of their mineralogical trends. These objects are probably very loose collections of weakly aggregated ices and dust. The dust includes not only the carbon compounds associated with primitive materials, but also pre-solar grains and high-temperature silicates formed in the hotter regions of the solar system. Results from the Stardust mission show that crystalline silicates are abundant in cometary dust, and recent modeling work indicates that outward transport of high-temperature materials can occur near the mid-plane of nebular disks. This transport can easily mix dust silicate materials that have been heated, melted, or annealed in the inner regions of the solar nebula with hugely dissimilar materials including ices and pre-solar grains. One can envision that these materials then accreted in the outer regions of the nebula, with their very low relative velocities and low temperatures producing a very underdense fairy castle structure that could produce cometary and TNO porosities of 70% or more.

Note that in general, macroporosity does appear to increase as one travels further from the Sun (see Fig. 8). Likewise, the meteorites thought to come from the outer part of the asteroid belt, the carbonaceous chondrites, are on average more than twice as porous as the meteorites from the inner belt. One can envision a solar nebula where distance from the sun not only controls the composition of the material accreting into planets, but the physical nature of that material. In the inner nebula, the region that eventually produced the asteroids of the inner belt, physical conditions promoted the transformation of dusty aggregates into well-lithified

fragments which themselves may have experienced subsequent fracturing and possible catastrophic disruption and reaccretion. Further out, extremely high macroporosities are the rule.

Do the TNOs and Oort-cloud comet nuclei represent primordial, highly uncompressed dust aggregates dating from the initial phases of the solar nebula? Or are they re-processed, highly pulverized bodies? Or does their high macroporosity suggest that they were originally formed with some primordial ice of high abundance and extremely high volatility, perhaps pure methane ice, that has since sublimated and escaped? Curiously, our study of meteorite density and porosity has ultimately led us to raise such new and intriguing questions about the structure of bodies which no meteorites themselves have sampled.

5. Summary and conclusions

Non-destructive, non-contaminating, and relatively simple procedures can measure the bulk density, grain density, and porosity of meteorites. Such measurements provide important clues to the nature of the physical processes that formed and evolved both the meteorites themselves and their parent bodies. The best-studied group of meteorites are the ordinary chondrites; on the basis of several hundred measurements one can conclude that the porosity of all these samples average just under 10% (for unweathered falls), for both brecciated and unbrecciated samples, across all metamorphic grades, all shock states, and all classes (though the L chondrites may be a few percentage points less porous, on average, than the H and LL types). In these meteorites, the porosity appears to result from the passage of shocks through the samples; little or none of the porosity in most ordinary chondrites is due to incomplete compaction of the primordial material. By contrast, most carbonaceous meteorites are much more porous, typically 20% or higher. The location and nature of this porosity is still not clear, as much of it is not easily visible in electron microscope backscatter images. Exceptions to this high porosity rate among carbonaceous meteorites are in CO finds and reduced CV meteorites, although these trends are based on only a handful of measurements so far. No robust statements can be made yet for the other types of meteorites, because too few have been measured systematically.

Compared to the meteorites, the bulk densities of most small solar system bodies indicates that they must have extensive macroporosity, with interiors that are either significantly fractured or piles of rubble. Typical S-type asteroids range from 20% to 30% macroporous; darker C-type asteroids can be 40–60% macroporous; and icy bodies such as comets and small TNOs may be as much as 85% macroporous. This range of interior structures, where macroporosity appears to increase with distance from the sun, combined with the well-known compositional zoning in the asteroid belt (ranging from S to C to icy as one goes further away from the sun) provides insights into the nature of accretion and collisions in the early solar system.

Future work in meteorite density and porosity, and its possible implications for our understanding of solar system evolution, will occur in four general areas. Most clearly, the first task is to collect more data on more types of meteorites currently undersampled. Many more samples of C and E chondrites, all kinds of achondrites, and stony-iron (especially mesosiderite) meteorites must be measured to confirm the trends hinted at in the data so far and to unveil new systematic trends. But even among the ordinary chondrites, more data need to be taken on samples with shock states of 1, 5 and 6, petrographic grade 3, and multiple samples at a variety of sizes for meteorite showers.

The second direction of future research will be to determine exactly where the porosity is located in meteorites other than the ordinary chondrites. Is it correct to assume that the enstatite chondrite and primitive achondrite porosity is also due primarily to shock-induced microcracks? Do many achondrites have vesicles unseen by helium pycnometry? Where is the porosity of highly porous carbonaceous chondrites and low-shock ordinary chondrites located? In connection with this task will be understanding exactly what happens, both chemically and physically, in the terrestrial weathering of meteorites that do not have abundant metallic iron, such as the already oxidized carbonaceous meteorites or the essentially metal-free basaltic achondrites.

The third goal is to understand the formation and evolution of the fabric of the meteorites themselves. What turned the dust in the gas of a solar nebula into the well-compacted rocky material that directly, or in the form of relithified breccias, makes up the ordinary chondrites? Did carbonaceous chondrites experience a different lithification history? In order to test theories of lithification, we need to have theories to test. While the lithification of breccias is well understood (Bischoff et al., 1983) the earlier process of turning dust into rock is still a very open question. Sandstones, perhaps our best terrestrial analogy for the physical structure of chondrites, are lithified as a result of high pressures, high temperatures, or the action of water; but the environments where meteoritic material could experience any of these conditions is highly limited. Clearly impacts can provide both heat and pressure, and thus the lithification environment may well be tied to the collisional environment of the parent bodies. Thus our discussion of the ''stratigraphic sequence'' of asteroid compositions and physical structure may well be tied into variations in

both the degree and nature of the lithification processes among the different meteorite classes.

In this review we have emphasized connecting the physical nature of meteorites with the physical nature of their parent bodies to deduce a stratigraphic sequence within the small body population of the solar system and, by inference, infer the nature of events in the solar nebula which could account for that sequence. This choice of emphasis arises from the authors' own background as both geologists and astronomers; and our interpretation of those deductions is still at a very early stage. But we wish to emphasize that meteorite density and porosity measurements also have other significant implications for the understanding of individual meteorite parent bodies. Are all asteroids "rubble piles" or are some merely highly fractured coherent bodies? Is the high macroporosity seen in outer solar system bodies a primordial artifact of an incompletely lithified dusty accretion? Our conclusion that the ubiquitous porosity (in ordinary chondrites at least) is primarily due to shock events should also lead impact modelers to think more deeply about how shock waves are emplaced and transmitted in what are, today, highly macroporous parent bodies.

Our stratigraphic sequence itself is based on composition and density data for the asteroids that are still highly uncertain. Future work, both ground and spacecraft based, will be needed to expand and improve these data. Thus we look forward to the results of missions such as the Dawn, Rosetta, and New Horizons, and spacecraft still to be planned and launched. But we note that interpreting the results of those spacecraft will continue to require careful measurements of meteorite samples, already in our collections, here on Earth.

Acknowledgments

The authors are indebted to Phil Bland, Sara Russell, and William Bottke for their insights and helpful discussions. The database used in this review includes a large number of samples whose data were provided by Tomas Kohout of the University of Helsinki and Phil McCausland of the University of Western Ontario; we are grateful for their enthusiastic cooperation in sharing their data and their insights. The MetBase computer database of Jörn Koblitz was an invaluable aid to the analysis of the meteorite data. We thank Associate Editor Klaus Keil for soliciting this paper and for extensive editorial suggestions. The work of Britt and Macke was supported by NASA grants NNG06GG62G from the Planetary Geology and Geophysics Program and NNG05GC35G from the Discovery Data Analysis Program.

References

Abe, S., Mukai, T., Hirata, N., Barnouin-Jha, O.S., Cheng, A.F., Demura, H., Gaskell, R.W., Hashimoto, T., Hiraoka, K., Honda, T., Kubota, T., Matsuoka, M., Mizuno, T., Nakamura, R., Scheeres, D.J., Yoshikawa, M., 2006. Mass and local topography measurements of Itokawa by Hayabusa. Science 312, 1344–1347.

A'Hearn, M.F., Belton, M.J.S., Delamere, W.A., Kissel, J., Klaasen, K.P., McFadden, L.A., Meech, K.J., Melosh, H.J., Schultz, P.H., Sunshine, J.M., Thomas, P.C., Veverka, J., Yeomans, D.K., Baca, M.W., Busko, I., Crockett, C.J., Collins, S.M., Desnoyer, M., Eberhardy, C.A., Ernst, C.M., Farnham, T.L., Feaga, L., Groussin, O., Hampton, D., Ipatov, S.I., Li, J.Y., Lindler, D., Lisse, C.M., Mastrodemos, N., Owen Jr., W.M., Richardson, J.E., Wellnitz, D.D., White, R.L., 2005. Deep impact: excavating comet Tempel 1. Science 310, 258–264.

Alexayeve, K.N., 1958. Physical properties of stony meteorites and their interpretation based on the hypothesis on the origin of meteorites. Meteritika 16, 67–77.

Ash, R.D., Pillinger, C.T., 1995. Carbon, nitrogen and hydrogen in Saharan chondrites: the importance of weathering. Meteoritics 30, 85–92.

Asphaug, E., Benz, W., 1996. Size, density, and structure of comet Shoemaker-Levy 9 inferred from the physics of tidal breakup. Icarus 121, 225–248.

Bange, J., 1998. An estimation of the mass of asteroid 20-Massalia derived from the Hipparcos minor planets data. Astron. Astrophys. 340, L1–L4.

Barshay, S.S., Lewis, J.S., 1976. Chemistry of primitive solar material. Annu. Rev. Astron. Astrophys. 14, 81–94.

Bischoff, A., Rubin, A.E., Keil, K., Stöffler, D., 1983. Lithification of gas-rich chondrite regolith breccias by grain boundary and localized shock melting. Earth Planet. Sci. Lett. 66, 1–10.

Bland, P.A., Berry, F.J., Smith, T.B., Skinner, S.J., Pillinger, C.T., 1996. The flux of meteorites to the Earth and weathering in hot desert ordinary chondrite finds. Geochim. Cosmochim. Acta 60, 2053–2059.

Bland, P.A., Sexton, A.S., Jull, A.J.T., Bevan, A.W.R., Berry, F.J., Thornley, D.M., Astin, T.R., Britt, D.T., Pillinger, C.T., 1998. Climate and rock weathering: a study of terrestrial age dated ordinary chondritic meteorites from hot desert regions. Geochim. Cosmochim. Acta 62, 3169–3184.

Blum, J., Schräpler, R., Davidsson, B., Trigo-Rodríguez, J.M., 2006. The physics of protoplanetesimal dust agglomerates. I. Mechanical properties and relations to primitive bodies in the solar system. Astrophys. J. 652, 1768–1781.

Bottke, W.F., Vokrouhlickỳ, D., Rubincam, D.P., Brož, M., 2002. Dynamical evolution of asteroids and meteoroids using the Yarkovsky effect. In: Bottke, W., Cellino, A., Paolicchi, P., Binzel, R. (Eds.), Asteroids III. University of Arizona Press, Tucson, AZ, pp. 395–408.

Bowden, K.E., 2002. Effects of loading path on the shock metamorphism of porous quartz: an experimental study. Ph.D. Thesis, University of London, 228pp.

Britt, D.T., Consolmagno, G.J., 2000. The porosity of dark meteorites and the structure of low-albedo asteroids. Icarus 146, 213–219.

Britt, D.T., Consolmagno, G.J., 2003. Stony meteorite porosities and densities: a review of the data through 2001. Meteorit. Planet. Sci. 38, 1161–1180.

Britt, D.T., Yeomans, D.K., Housen, K.R., Consolmagno, G.J., 2002. Asteroid porosity and structure. In: Bottke, W., Cellino, A., Paolicchi, P., Binzel, R. (Eds.). University of Arizona Press, Tucson, pp. 485–500.

Brown, P.G., ReVelle, D.O., Tagliaferri, E., Hildebrand, A.R., 2002. An entry model for the Tagish Lake fireball using seismic, satellite and infrasound records. Meteorit. Planet. Sci. 37, 661–675.

Brown, M.E., Trujillo, C.A., Rabinowitz, D.L., 2005. Discovery of a planetary-sized object in the scattered Kuiper belt. Astrophys. J. 635, L97–L100.

Brown, M.E., Schaller, E.L., 2007. The mass of dwarf planet Eris. Science 316, 1585.

Buie, M.W., Grundy, W.M., Young, E.F., Young, L.A., Stern, S.A., 2006. Orbits and photometry of Pluto's satellites: Charon, S/2005 P1, and S/2005 P2. Astron. J. 132, 290–298.

Bus, S.J., Binzel, R.P., 2002. Phase II of the small main-belt asteroid spectroscopic survey: a feature-based taxonomy. Icarus 158, 146–177.

Bus, S.J., Vilas, F., Barucci, M.A., 2002. Visible-wavelength spectroscopy of asteroids. In: Bottke, W., Cellino, A., Paolicchi, P., Binzel, R. (Eds.), Asteroids III. University of Arizona Press, Tucson, AZ, pp. 169–182.

Campins, H., Swindle, T.D., 1998. Expected characteristics of cometary meteorites. Meteorit. Planet. Sci. 33, 1201–1211.

Cellino, A., 2000. Minor bodies: spectral gradients and relationships with meteorites. Space Sci. Rev. 92, 397–412.

Consolmagno, G.J., Britt, D.T., 1998. The density and porosity of meteorites from the Vatican collection. Meteorit. Planet. Sci. 33, 1231–1240.

Consolmagno, G.J., Britt, D.T., Stoll, C.P., 1998. The porosities of ordinary chondrites: models and interpretation. Meteorit. Planet. Sci. 33, 1221–1230.

Consolmagno, G.J., Macke, R.J., Rochette, P., Britt, D.T., Gattacceca, J., 2006a. Density, magnetic susceptibility, and the characterization of ordinary chondrite falls and showers. Meteorit. Planet. Sci. 41, 331–342.

Consolmagno, G.J., Tegler, S.C., Romanishin, W., Britt, D.T., 2006b. Shape, spin, and the structure of asteroids, centaurs, and Kuiper belt objects (abstract). Lunar Planet. Sci. XXXVII, abstract #1222.

Consolmagno, G.J., Wignarajah, D.P., Britt, D.T., 2007. Bulk densities of assorted CK chondrites, primitive achondrites, and Bencubbin (abstract). Meteorit. Planet. Sci. 42, A33.

Corrigan, C.M., Zolensky, M.E., Dahl, J., Long, M., Weir, J., Sapp, C., 1997. The porosity and permeability of chondritic meteorites and interplanetary dust particles. Meteoritics 32, 509–516.

Davidsson, B.J.R., Gutiérrez, P.J., 2003. An estimate of the nucleus density of comet 19P/Borrelly (abstract). Bull. A. A. S. 35, 969.

Davidsson, B.J.R., Gutiérrez, P.J., 2006. Non-gravitational force modeling of Comet 81P/Wild 2. I. A nucleus bulk density estimate. Icarus 180, 224–242.

DeCarli, P.S., Bowden, E., Seaman, L., 2001. Shock-induced compaction and porosity in meteorites (abstract). Meteorit. Planet. Sci. Suppl. 36, A47.

Descamps, P., Marchis, F., Michalowski, T., Vachier, F., Colas, F., Berthier, J., Assafin, M., Dunckel, P.B., Polinska, M., Pych, W., Hestroffer, D., Miller, K.P.M., Vieira-Martins, R., Birlan, M., Teng-Chuen-Yu, J.-P., Peyrot, A., Payet, B., Dorseuil, J., Léonie, Y., Dijoux, T., 2007. Figure of the double Asteroid 90 Antiope from adaptive optics and lightcurve observations. Icarus 187, 482–499.

Emery, J.P., Cruikshank, D.O., van Cleve, J., 2006. Thermal emission spectroscopy (5.2–38 μm) of three Trojan asteroids with the Spitzer Space Telescope: detection of fine-grained silicates. Icarus 182, 496–512.

Flynn, G.J., Klock, W., 1998. Densities and porosities of meteorites: implications for the porosities of asteroids (abstract). Lunar Planet. Sci. XXIX, abstract 1112.

Flynn, G.J., Moore, L.B., Klock, W., 1999. Density and porosity of stone meteorites: implications for the density, porosity, cratering, and collisional disruption of asteroids. Icarus 142, 97–105.

Fulchignoni, M., Delasnti, A., Barucci, M.A., Birlan, M., 2003. Toward a taxonomy of the Edgweorth–Kuiper objects: a multivariate approach. Earth Moon Planets 92, 243–250.

Gaffey, M.J., Burbine, T.H., Binzel, R.P., 1993. Asteroid spectroscopy: progress and perspectives. Meteoritics 28, 161–187.

Gaffey, M.J., Cloutis, E.A., Kelley, M.S., Reed, K.L., 2002. Mineralogy of asteroids. In: Bottke, W., Cellino, A., Paolicchi, P., Binzel, R. (Eds.), Asteroids III. University of Arizona Press, Tucson, AZ, pp. 183–204.

Gladman, B.J., Migliorini, F., Morbidelli, A., Zappala, V., Michel, P., Cellino, A., Froeschlé, C., Levison, H.F., Bailey, M., Duncan, M., 1997. Dynamical lifetimes of objects injected into asteroid belt resonances. Science 277, 197–201.

Gounelle, M., Zolensky, M., 2001. A terrestrial origin for sulfate veins in CI chondrites. Meteorit. Planet. Sci. 36, 1321–1329.

Gradie, J., Tedesco, E., 1982. Compositional structure of the asteroid belt. Science 216, 1405–1407.

Greenwood, R.C., Franchi, I.A., 2004. Alteration and metamorphism of CO3 chondrites: evidence from oxygen and carbon isotopes. Meteorit. Planet. Sci. 39, 1823–1838.

Grundy, W.M., Stansberry, J.A., Noll, K.S., Stephens, D.C., Kern, S.D., Spencer, J.R., Trilling, D.E., Cruikshank, D.P., Levison, H.F., 2006. The orbit, mass, size, albedo, and density of the binary Centaur (65489) 2003 FX128 (abstract). Bull. Am. Astron. Soc. 38, 557.

Grundy, W.M., Stansberry, J.A., Noll, K.S., Stephens, D.C., Trilling, D.E., Kern, S.D., Spencer, J.R., Cruikshank, D.P., Levison, H.F., 2007. The orbit, mass, size, albedo, and density of (65489) Ceto/Phorcys: a tidally evolved binary Centaur. Icarus 191, 286–297.

Guskova, E.G., 1985. Magnetic properties of enstatite chondrites. Meteoritika 44, 111–118 (in Russian).

Heiken, G.H., Vaniman, D.T., French, B.M., 1991. Lunar Sourcebook: A User's Guide to the Moon. Cambridge

University Press and Lunar and Planetary Institute, Houston, TX, 736pp.

Henderson, E.P., Perry, S.H., 1954. A discussion of the densities of iron meteorites. Geochim. Cosmochim. Acta 6, 221–240.

Hildebrand, A.R., McCausland, P.J.A., Brown, P.G., Longstaffe, F.J., Russell, S.D.J., Tagliaferri, E., Wacker, J.F., Mazur, M.J., 2006. The fall and recovery of the Tagish Lake meteorite. Meteorit. Planet. Sci. 41, 407–431.

Hunt, S.M., Oppenheim, M., Close, S., Brown, P.G., McKeen, F., Mindardi, M., 2003. Determination of the meteroid velocity distribution at the Earth using high-gain radar. Icarus 168, 34–42.

Joswiak, D.J., Brownlee, D.E., Pepin, R.O., Schlutter, D.J., 2007. Densities and mineralogy of cometary and asteroidal interplanetary dust particles collected in the stratosphere. In: Krueger, H., Graps, A. (Eds.), Workshop on Dust in Planetary Systems (ESA SP-643), pp. 141–144.

Keil, K., 1962. Quantitativ-erzmikroskopische Integrationsanalyse der Chondrite. Chem. Erde 22, 281–348.

Kitts, K., Lodders, K., 1998. Survey and evaluation of eucrite bulk compositions. Meteorit. Planet. Sci. 33 (Suppl.), 197–213.

Kohout, T., Elbra, T., Pesonen, L.J., Schnabl, P., Slechta, S., 2006. Study of the physical properties of meteorites using mobile laboratory facility (abstract). Lunar Planet. Sci. XXXVII, abstract 1607.

Krot, A.N., Scott, E.R.D., Zolensky, M.E., 1995. Mineralogical and chemical modification of components in CV3 chondrites: nebular or asteroidal processing? Meteoritics 30, 748–775.

Kukkonen, I., Pesonen, L.J., 1983. Classification of meteorites by petrophysical methods. Bull. Geol. Soc. Finland 55, 157–177.

Lacerda, P., Jewitt, D.C., 2007. Densities of solar system objects from their rotational light curves. Astronom. J. 133, 1393–1408.

Lebofsky, L.A., Jones, T.D., Owensby, P.D., Feierberg, M.A., Consolmagno, G.J., 1990. The nature of low albedo asteroids from 3-μm spectrophotometry. Icarus 83, 16–26.

Levison, H.F., Morbidelli, A., 2003. The formation of the Kuiper belt by the outward transport of bodies during Neptune's migration. Nature 426, 419–421.

Lewis, J.S., 1974. The temperature gradient in the solar nebula. Science 186, 440–443.

Licandro, J., Pinilla-Alonso, N., Pedani, M., Oliva, E., Tozzi, G.P., Grundy, W.M., 2006. The methane ice rich surface of large TNO 2005 FY9: a Pluto-twin in the trans-Neptunian belt? Astron. Astrophys. 445, L35–L38.

Lippolt, H.J., Weigel, E., 1988. ^{4}He diffusion in ^{40}Ar retentive minerals. Geochim. Cosmochim. Acta 52, 1449–1458.

Lisse, C.M., A'Hearn, M.F., Hauser, M.G., Kelsall, T., Lien, D.J., Moseley, S.H., Reach, W.T., Silverberg, R.F., 1998. Infrared observations of comets by COBE. Astrophys. J. 496, 971–991.

Lodders, K., 1998. A survey of SNC meteorite whole-rock compositions. Meteorit. Planet. Sci. 33 (Suppl.), 183–190.

Love, S.G., Joswiak, D.J., Brownlee, D.E., 1994. Densities of stratospheric micrometeorites. Icarus 111, 227–236.

Macke, R., 2007. Bulk and grain densities of Allende and other carbonaceous chondrites (abstract). Bull. A. A. S., DPS abstract ♯20.05.

MacPherson, G.J., Krot, A.N., 2002. Distribution of Ca–Fe-silicates in CV3 chondrites: possible controls by parent-body compaction (abstract). Meteorit. Planet. Sci. Suppl. 37, A91.

Magri, C., Consolmagno, G.J., Ostro, S.J., Benner, L.A.M., Beeny, B.R., 2001. Radar constraints on asteroid regolith properties using 433 Eros as ground truth. Meteorit. Planet. Sci. 36, 1697–1709.

Marchis, F., Descamps, P., Hestroffer, D., Berthier, J., 2005. Discovery of the triple asteroidal system 87 Sylvia. Nature 436, 822–824.

Marchis, F., Hestroffer, D., Descamps, P., Berthier, J., Bouchez, A.H., Campbell, R.D., Chin, J.C.Y., van Dam, M.A., Hartman, S.K., Johansson, E.M., Lafon, R.E., Le Mignant, D., de Pater, I., Stomski, P.J., Summers, D.M., Vachier, F., Wizinovich, P.L., Wong, M.H., 2006. A low density of 0.8 g cm^{-3} for the Trojan binary asteroid 617 Patroclus. Nature 439, 565–567.

Margot, J.L., Brown, M.E., 2003. A low-density M-type asteroid in the main belt. Science 300, 1939–1942.

Margot, J.L., Nolan, M.C., Benner, L.A.M., Ostro, S.J., Jurgens, R.F., Giorgini, J.D., Slade, M.A., Campbell, D.B., 2002. Binary asteroids in the near-Earth object population. Science 296, 1445–1448.

Matsui, T., Hamano, Y., Honda, M., 1980. Porosity and compressional-wave velocity measurement of Antarctic meteorites. Mem. Natl. Inst. Polar Res. (special issue) 17, 268–275.

McBride, K.M., 2002. Statistical comparisons of Antarctic meteorites and falls (abstract). LPSC XXXIII, abstract ♯1323.

McCausland, P.J.A., Samson, C., Deslauriers, A., 2007. Bulk densities of meteorites via visible light 3D laser imaging (abstract). Meteorit. Planet. Sci. Suppl. 42, 5066.

McSween, H.Y., Bennett III, M.E., Jarosewich, E., 1991. The mineralogy of ordinary chondrites and implications for asteroid spectrophotometry. Icarus 90, 107–116.

Melosh, H.J., Ryan, E.V., 1997. Asteroids: shattered but not dispersed. Icarus 129, 562–564.

Merline, W.J., Weidenschilling, S.J., Durda, D.D., Margot, J.L., Pravec, P., Storrs, A.D., 2002. Asteroids do have satellites. In: Bottke, W., Cellino, A., Paolicchi, P., Binzel, R. (Eds.), Asteroids III. University of Arizona Press, Tucson, AZ, pp. 289–312.

Miyamoto, M., Fujii, N., Ito, K., Kobayashi, Y., 1982. The fracture strength of meteorites: its implications for their fragmentation. Mem. Natl. Inst. Polar Res. (special issue) 25, 331–342.

Moore, L.B., Flynn, G.J., Klock, W., 1999. Density and porosity measurements on meteorites: implications for the porosities of asteroids (abstract). Lunar Planet. Sci. XXX, abstract 1607.

Morbidelli, A., Froeschlé, C., 2003. Origin and dynamical transport of near-Earth asteroids and meteorites. In: Impacts on Earth, The Spring School of Astronomy and Astrophysics of Goutelas, Lecture Notes in Physics, vol. 505, pp. 31–53.

Morbidelli, A., Bottke, W.F., Froeschlé, C., Michel, P., 2002. Origin and evolution of near-Earth objects. In: Bottke, W., Cellino, A., Paolicchi, P., Binzel, R. (Eds.), Asteroids III. University of Arizona Press, Tucson AZ, pp. 409–422.

Morbidelli, A., Tsiganis, K., Crida, A., Levison, H.F., Gomes, R., 2007. Dynamics of the giant planets of the solar system in the gaseous protoplanetary disk and their relationship to the current orbital architecture. Astronom. J. 134, 1790–1798.

Mottola, S., Lahulla, F., 2000. Mutual eclipse events in asteroidal binary system 1996 FG3: observations and a numerical model. Icarus 146, 556–567.

Neish, C.D., Nolan, M.C., Howell, E.S., Rivkin, A.S., 2003. Radar observations of binary asteroid 5381 Sekhmet (abstract). Bull. A. A. S. 35, 1421.

Nolan, M.C., Margot, J.-L., Howell, E.S., Benner, L.A.M., Ostro, S.J., Jurgens, R.F., Giorgini, J.D., Campbell, D.B., 2001. Radar observations of near-Earth asteroids 2000 UG11 and 2000 UK11 (abstract). In: Lunar and Planetary Science Conference XXXII, abstract 2055.

Noll, K.S., Grundy, W.M., Stephens, D.C., Levison, H.F., Kern, S.D., 2007. Evidence for two populations of classical trans-Neptunian objects: the strong inclination dependence of classical binaries. Icarus, in press, doi:10.1016/j.icarus.2007.10.022.

Ostro, S.J., Hudson, R.S., Benner, L.A.M., Giorgini, J.D., Magri, C., Margot, J.L., Nolan, M.C., 2002. Asteroid radar astronomy. In: Bottke, W., Cellino, A., Paolicchi, P., Binzel, R. (Eds.), Asteroids III. University of Arizona Press, Tucson, AZ, pp. 151–168.

Ostro, S.J., Margot, J-L., Benner, L.A.M., Giorgini, J.D., Scheeres, D.J., Fahnestock, E.G., Broschart, S.B., Bellerose, J., Nolan, M.C., Magri, C., Pravec, P., Scheirich, P., Rose, R., Jurgens, R.F., De Jong, E.M., Suzuk, S., 2006. Radar imaging of binary near-Earth asteroid (66391) 1999 KW4. Science 314, 1276–1280.

Person, M.J., Elliot, J.L., Gulbis, A.A.S., Pasachoff, J.M., Babcock, B.A., Souza, S.P., Gangestad, J., 2006. Charon's radius and density from the combined data sets of the 2005 July 11 occultation. Astron. J. 132, 1575–1580.

Pesonen, L., Terho, M., Kukkonen, I.T., 1993. Physical properties of 368 meteorites: implications for meteorite magnetism and planetary geophysics. In: Proceedings of the NIPR Symposium of Antarctic Meteorites, vol. 6, pp. 401–416.

Petit, J.-M., Durda, D.D., Greenberg, R., Hurford, T.A., Geissler, P.E., 1997. The long-term dynamics of Dactyl's orbit. Icarus 130, 177–197.

Pravec, P., 2006. and 57 co-authors Icarus 181, 63–93.

Rabinowitz, D.L., Toutellotte, S., Brown, M.E., Trujillo, C., 2005. Photometric observations of a very bright TNO with an extraordinary lightcurve (abstract). Bull. A. A. S. 37, 746.

Rabinowitz, D.L., Barkume, K., Brown, M.E., Roe, H., Schwartz, M., Tourtellotte, S., Trujillo, C., 2006. Photometric observations constraining the size, shape, and albedo of 2003 EL61, a rapidly rotating, Pluto-sized object in the Kuiper belt. Astrophys. J. 639, 1238–1251.

Richardson, J.E., Melosh, H.J., Lisse, C.M., Carcich, B., 2007. A ballistics analysis of the Deep Impact ejecta plume: determining comet Tempel 1's gravity, mass, and density. Icarus 190, 357–390.

Rivkin, A.S., Clark, B.E., Britt, D.T., Lebofsky, L.A., 1997. Infrared spectrophotometry of the NEAR flyby target 253 Mathilde. Icarus 127, 255–257.

Rivkin, A.S., Trilling, D.E., Plassman, J.H., Brown, R.H., Bell III, J.F., 1999. Infrared spectrophotometry of Phobos (abstract). Bull. A. A. S. DPS, abstract ♯04.02.

Rivkin, A.S., Binzel, R.P., Sunshine, J., Bus, S.J., Burbine, T.H., Saxena, A., 2004. Infrared spectroscopic observations of 69230 Hermes 1937 UB: possible unweathered end-member among ordinary chondrite analogs. Icarus 172, 408–414.

Rochette, P., Sagnotti, L., Consolmagno, G., Denise, M., Folco, L., Osete, M., Pesonen, L., 2003. Magnetic classification of stony meteorites: 1. Ordinary chondrites. Meteorit. Planet. Sci. 38, 251–268.

Rochette, P., Gattacceca, J., Bonal, L., Bourot-Denise, M., Chevrier, V., Clerc, J.-P., Consolmagno, G., Folco, L., Gounelle, M., Kohout, T., Pesonen, L., Quirico, E., Sagnotti, L., Skripnik, A., 2008. Magnetic classification of stony meteorites: 2. Non-ordinary chondrites. Meteorit. Planet. Sci., in press.

Roush, T.L., Cruikshank, D.P., Pollack, J.B., Young, E.F., Bartholomew, M.J., 1996. Near infrared spectral geometric albedos of Charon and Pluto: constraints on Charon's surface composition. Icarus 119, 214–218.

Sears, D.W., Kallemeyn, G.W., Wasson, J.T., 1982. The compositional classification of chondrites: II. The enstatite chondrite groups. Geochim. Cosmochim. Acta 46, 597–608.

Smith, D.E., Lemoine, F.G., Zuber, M.T., 1995. Simultaneous estimation of the masses of Mars, Phobos, and Deimos using spacecraft distant encounters. Geophys. Res. Lett. 22, 2171–2174.

Smith, D.L., Samson, C., Herd, R., Deslauriers, A., Sink, J.-E., Christie, I., Ernst, R.E., 2006. Measuring the bulk density of meteorites nondestructively using three-dimensional laser imaging. J. Geophys. Res. 111, E10002.

Spencer, J.R., Stansberry, J.A., Grundy, W.M., Noll, K.S., 2006. A low density for binary Kuiper belt object (26308) 1998 SM165 (abstract). Bull. A. A. S. 38, 546.

Stacy, F.D., Lovering, J.F., Parry, L.G., 1961. Thermomagnetic properties, natural magnetic moments, and magnetic anisotropies of some chondritic meteorites. J. Geophys. Res. 66, 1523–1534.

Standish, E.M., 2001. JPL Interoffice Memorandum 312. F-01-006 dated April 11, 2001.

Standish, E.M., Fienga, A., 2002. Accuracy limit of modern ephermides imposed by the uncertainties in asteroid masses. Astron. Astrophys. 384, 322–328.

Stansberry, J.A., Grundy, W.M., Margot, J.L., Cruikshank, D.P., Emery, J.P., Rieke, G.H., Trilling, D.T., 2006. The albedo, size, and density of binary Kuiper belt object (47171) 1999 TC36. Astrophys. J. 643, 556–566.

Strait M.M., Consolmagno G.J., 2002a. Microcrack porosity in the L-LL meteorite Knyahinya: how homogeneous? Lunar Planet. Sci. XXXIII, 1711 (abstract).

Strait, M.M., Consolmagno, G.J., 2002b. The nature and origin of meteorite porosity: evidence from thin section analysis (abstract). Meteorit. Planet. Sci. 37, A137.

Strait, M.M., Consolmagno, G.J., 2005. Validation of methods used to determine microcrack porosity in meteorites (abstract). LPSC XXXVI, abstract 2073.

Swindle, T.D., Campins, H., 2004. Do comets have chondrutes and CAIs? Evidence from the Leonid meteors. Meteorit. Planet. Sci. 39, 1733–1740.

Tedesco, E.F., Veeder, G.J., Fowler, J.W., Chillemi, J.R., 1992. The IRAS minor planet survey. Phillips Laboratory Report PL-TR-92-2049.

Tegler, S.C., Romanishin, W., Consolmagno, G.J., 2003. A primordial origin for the colors of Kuiper belt objects. Ap. J. Lett. 599, L49–L52.

Tegler, S.C., Romanishin, W., Consolmagno, G.J., Rall, J., Worhatch, R., Nelson, M., Weidenschilling, S.J., 2005. The period of rotation, shape, density, and homogeneous surface color of the Centaur 5145 Pholus. Icarus 175, 390–396.

Tegler, S.C., Grundy, W.M., Romanishin, W., Consolmagno, G.J., Mogren, K., Vilas, F., 2007. Optical spectroscopy of the large Kuiper belt objects 136472 (2005 FY9) and 136108 (2003 EL61). Astronom. J. 133, 526–530.

Tegler, S.C., Grundy, W.M., Vilas, F., Romanishin, Wl., Cornelison, D., Consolmagno, G.J., 2008. Evidence of N2-Ice on the surface of the icy dwarf planet 136472 (2005 FY9). Icarus, in press. (arXiv:0801.3115).

Terho, M., Pesonen, L.J., Kukkonen, I.T., 1991. The petrophysical classification of meteorites: new results. Geological Survey of Finland Report Q29, 1/91/1.

Terho, M., Pesonen, L.J., Kukkonen, I.T., Bukovanská, M., 1993. The petrophysical classification of meteorites. Studia Geophys. Geod. 37, 65–82.

Trull, T.W., Kurz, M.D., Jenkins, W.J., 1991. Diffusion of cosmogenic ^{3}He in olivine and quartz: implications for surface exposure dating. Earth Planet. Sci. Lett. 103, 241–256.

Urey, H.C., 1952. The Planets: Their Origin and Development. Yale University Press, New Haven, 245pp.

Viateau, B., 2000. Mass and density of asteroids (16) Psyche and (121) Hermione. Astron. Astrophys. 354, 725–731.

Viateau, B., Rapaport, M., 1997. The Bordeaux meridian observations of asteroids. First determination of the mass of (11) Parthenope. Astron. Astrophys. 320, 652–658.

Wilkison, S.L., Robinson, M.S., 2000. Bulk density of ordinary chondrite meteorites and implications for asteroidal internal structure. Meteorit. Planet. Sci. 35, 1203–1213.

Wilkison, S.L., Robinson, M.S., Thomas, P.C., Veverka, J., McCoy, T.J., Murchie, S.L., Prockter, L.M., Yeomans, D.K., 2002. An estimate of Eros's porosity and implications for internal structure. Icarus 155, 94–103.

Wilkison, S.L., McCoy, T.J., McCamant, J.E., Robinson, M.S., Britt, D.T., 2003. Porosity and density of ordinary chondrites: Clues to the formation of friable and porous ordinary chondrites. Meteorit. Planet. Sci. 38, 1533–1546.

Wilson, L., Keil, K., Love, S.J., 1999. The internal structures and densities of asteroids. Meteorit. Planet. Sci. 34, 479–483.

Yeomans, D.K., Barriot, J.-P., Dunham, D.W., Farquhar, R.W., Giorgini, J.D., Helfrich, C.E., Konopliv, A.S., McAdams, J.V., Miller, J.K., Owen Jr., W.M., Scheeres, D.J., Synnott, S.P., Williams, B.G., 1997. Estimating the mass of asteroid 253 Mathilde from tracking data during the NEAR flyby. Science 278, 2106–2109.

Yeomans, D.K., Antreasian, P.G., Barriot, J.-P., Chesley, S.R., Dunham, D.W., Farquhar, R.W., Giorgini, J.D., Helfrich, C.E., Konopliv, A.S., McAdams, J.V., Miller, J.K., Owen Jr., W.M., Scheeres, D.J., Thomas, P.C., Veverka, J., Williams, B.G., 2000. Radio science results during the NEAR-shoemaker spacecraft rendezvous with eros. Science 289, 2085–2088.

Yomogida, K., Matsui, T., 1981. Physical properties of some Antarctic meteorites. Mem. Natl. Inst. Polar Res. (special issue) 20, 384–394.

Yomogida, K., Matsui, T., 1983. Physical properties of ordinary chondrites. J. Geophys. Res. 88, 9513–9533.